**Supporting Information**

# Rational Design of Poly(disulfide)s as a Universal Platform for Delivery of CRISPR/Cas9 Machineries towards Therapeutic Genome Editing

Jiajing Guo[a,#], Tao Wan[a,b#], Bowen Li[a], Qi Pan[a], Huhu Xin[a], Yayu Qiu[c], Yuan Ping[a,b*]

[a] College of Pharmaceutical Sciences, Zhejiang University, Hangzhou 310058, China

[b] Liangzhu Laboratory, Zhejiang University Medical Center, Hangzhou 311121, China

[c] Department of Chemistry, Zhejiang University, Hangzhou 310058, China

*Corresponding author: E-mail: pingy@zju.edu.cn (Y. Ping).

[#]The authors contributed equally to this work.

**Table of contents**

**Materials and Methods**

All chemicals were commercially available without further purification. Lipoic acid, 1,1'-carbonyldiimidazole (CDI), diethylenetriamine, L-Arginine methyl ester dihydrochloride, N, N-diisopropylethylamine (DIEA), ICG-NHS, polyethyleneimine (PEI MW: 25 kDa), N-acetyl-L-cysteine methyl ester, TEOA, 2-Iodoacetamide, Lipofectamine 2000 (Lipo 2000), Lipofectamine 3000 (Lipo 3000), Lipofectamine CRISPR MAX (C-MAX), Dulbecco's modified Eagle's medium (DMEM), RPMI 1640 were purchased from Sigma-Aldrich (USA). Fetal bovine serum (FBS) was purchased from ZhejiangTianhang Biotechnology Co.Ltd. (China). The 3-(4,5-dimethylthiazol-2-yl)-2,5-diphenyltetrazolium bromide (MTT) assay kit was obtained from MultiSciences (HangZhou). The label IT Nucleic Acid Labeling kit, CX-Rhodamine was purchased from Mirusbio (USA). The YOYO-1 Nucleic Acid Labeling kit was purchased from AAT Bioquest (USA). The protein release kit (BCA kit) was purchased from Beyotime (China). The dialysis tube (3500 Da, 2000 Da), mPEG-Thiol and PBS buffer were obtained from Solarbio Science & Technology Co., Ltd. (Beijing, China). T7 endonuclease 1 (T7E1) enzyme was purchased from GenScript (USA). The FastPure® cell/tissue DNA Isolation Mini Kit and FastPure® Gel DNA Extraction Mini Kit were purchased from Vazyme Biotech Co., Ltd (China). Ultrapure water was obtained from a Milli-Q system. The $^{1}H$ NMR and $^{13}C$ NMR spectra were carried out on a Bruker 400 MHz NMR spectrometer and were reported as chemical shifts (δ) in ppm relative to TMS (δ = 0). Proton spin multiplicities are reported as a singlet (s), doublet (d), triplet (t), quartet (q) and quintet (quint) with coupling constants (J) given in Hz, or multiplet (m). Mass spectra were recorded on a Shimadzu LC-MS mass spectrometer (LC-MS 2020). Transmission electron microscopy (TEM) was carried out on a transmission electron microscope (HT7700, Hitachi, Japan). Size and zeta potentials of the polyplexes were characterized by Malvern Nano ZS90. Confocal microscopy was performed on a Carl Zeiss, LSM-880 (Germany). The luciferase intensity was evaluated by vivo imaging system (IVIS® Spectrum, PerkinElmer). Gel permeation chromatography (GPC) analysis was performed on a Waters 1524 with a Superdex™ 75 10/300 GL column (GE, made in USA, flow 0.4 ml/min, eluent: 30% ACN in 0.1 M acetate buffer pH = 6.5) equipped with a Waters 2489 UV/Vis detector, the molecular weight standard samples purchased from Sigma (USA) including somatostatin (1638 Da), thymosin α1 (3108 Da), recombinant human insulin (5808 Da), ribonuclease A (13700 Da) and β-lactoglobulin (35000 Da), respectively. No unexpected or unusually high safety hazards were encountered.

**Synthesis procedures**

Synthesis of the **M1**

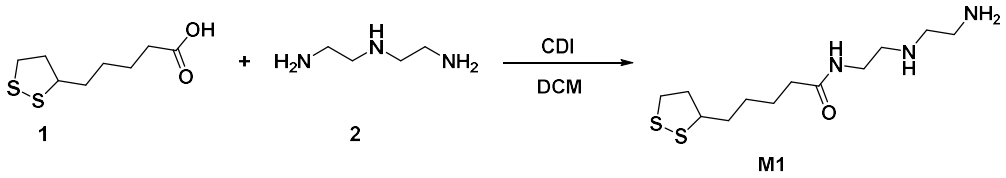


1 2 M1

Commercially available lipoic acid **1** (4.12 g, 20 mmol) and CDI (4.28 g, 26.4 mmol) were dissolved in dry DCM (100 ml). The solution was stirred at 0 °C, and diethylenetriamine **2** (DET, 16 g, 155 mmol) dissolved in dry DCM (30 ml) was added dropwise into aforementioned solution mixture at 0 °C. The reaction mixture continued to stir for 1 h at 0 °C and then was restored to room temperature for 1 h. The mixture was washed with brine (3 × 100 ml). The organic layer was dried over anhydrous $Na_2SO_4$ and concentrated under reduced pressure to yield **M1** as yellow oil (2.9 g, 50%). MS (ESI, MeOH): 292 ($[M+H]^+$). $^1$H NMR (400 MHz, DMSO) δ 7.90 (t, J = 5.6 Hz, 1H), 4.23 (q, J = 5.2 Hz, 1H), 3.69 – 3.59 (m, 1H), 3.43 – 3.32 (m, 1H), 3.29 – 3.14 (m, 8H), 3.14 – 3.06 (m, 2H), 2.52 – 2.39 (m, 1H), 2.09 (t, J = 7.4 Hz, 2H), 1.96 – 1.86 (m, 1H), 1.69 (s, 1H), 1.55 (ddd, J = 14.4, 8.2, 2.4 Hz, 3H), 1.43 – 1.32 (m, 2H).$^{13}$C NMR (101 MHz, DMSO) δ 172.75, 56.62, 55.41, 52.47, 49.08, 48.18, 38.60, 37.87, 35.67, 34.63, 28.85, 25.43.

Synthesis of the **M2**

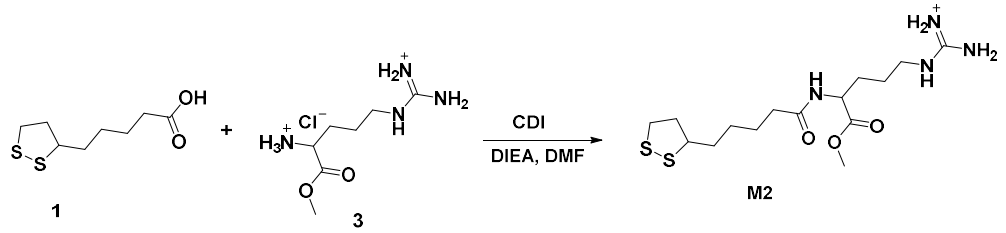


1 3 M2

Lipoic acid **1** (4.12 g, 20 mmol) and CDI (3.24 g, 20 mmol) were added in anhydrous DMF (50 ml), and the mixture was stirred at room temperature for 2 h. To a solution mixture of methyl L-arginine methyl ester dihydrochloride **3** (2.61 g, 10 mmol) and DIEA (1.74 µl, 10 mmol) in anhydrous DMF (40 ml), the activated lipoic acid was added and the solution mixture was further stirred at room temperature for 3.5 h. After that, the reaction mixture was added dropwise into $Et_2O$ (200 ml), and the resulted precipitate was centrifuged (2 min, 3000 rpm). The precipitate was collected and the obtained yellow oil was washed with MeOH/ $Et_2O$ mixture (1:2, 50 × 100 ml) for three times. The crude product was purified by flash silica gel column chromatography (DCM/MeOH = 50:1) to give **M2** as yellow oil (Cl salt, 3.39 g, 45%). MS (ESI, MeOH): 378 ($[M+H]^+$); $^1$H NMR (400 MHz, DMSO) δ 8.30 (t, J = 16.9 Hz, 1H), 7.87 (s, 1H), 7.55 – 7.23 (m, 1H), 7.07 (s, 1H), 4.21 (dd, J = 12.9, 8.4 Hz, 1H), 3.61 (d, J = 4.9 Hz, 4H), 3.23 – 3.13 (m, 3H), 3.13 – 3.05 (m, 3H), 2.41 (dd, J = 12.8, 6.3 Hz, 1H), 2.14 (t, J = 7.3 Hz, 2H), 1.91 – 1.79 (m, 1H), 1.76 – 1.58 (m, 3H), 1.52 (dt, J = 21.2, 7.1 Hz,

6H), 1.35 (dd, J = 15.3, 7.5 Hz, 2H). $^{13}$C NMR (101 MHz, DMSO) δ 173.00, 172.87, 157.46, 56.60, 52.26, 52.02, 49.03, 40.66, 38.56, 35.18, 34.55, 28.66, 28.63, 28.32, 25.61, 25.40.

Polymerization of DETs[1]

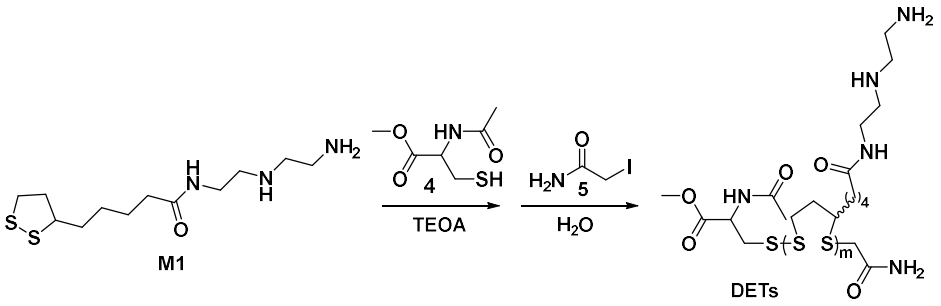


To a solution of initiator **4** (0.03 mM) in 2 ml TEOA buffer (1.0 M, pH = 7), **M1** solution (2.4 mM) in 10 ml TEOA buffer was added, and then the reaction mixture stirred vigorously under $N_2$ atmosphere. For polymerization, the sample was kept at room temperature with vigorous agitation. After a fixed period of time (30 min, 1.0 h, 1.5 h, 2.0 h, 2.5 h, 3.0 h), 2 ml of polymerization mixture was collected and was quenched in a solution of terminator **5** (2 mM) in water. The mixture was dialyzed in water for 7 days to yield poly(disulfide)s, including DET-1, DET-2, DET-3, DET-4, DET-5, DET-6, respectively.

Polymerization of CPDs

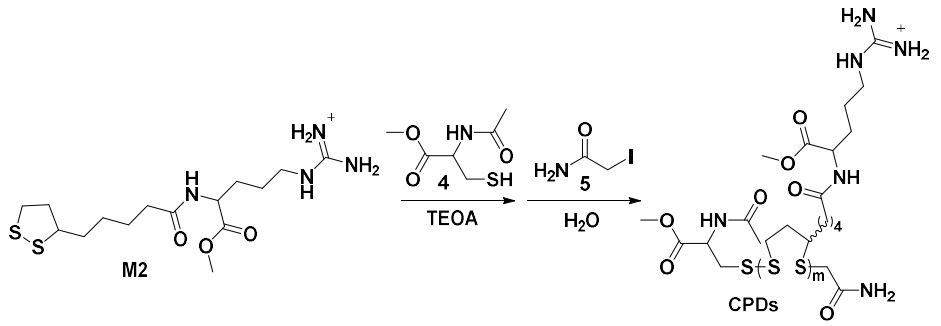


To a solution of initiator **4** (0.03 mM) in 2 ml TEOA buffer (1.0 M, pH = 7) was added in solution of **M2** (2.4 mM) in 10 ml TEOA buffer and then the reaction mixture stirred vigorously under $N_2$ atmosphere. For polymerization, the procedures of CPDs were same as DETs, obtaining CPD-1, CPD-2, CPD-3, CPD-4, CPD-5, CPD-6, respectively.

Polymerization of DET-CPDs

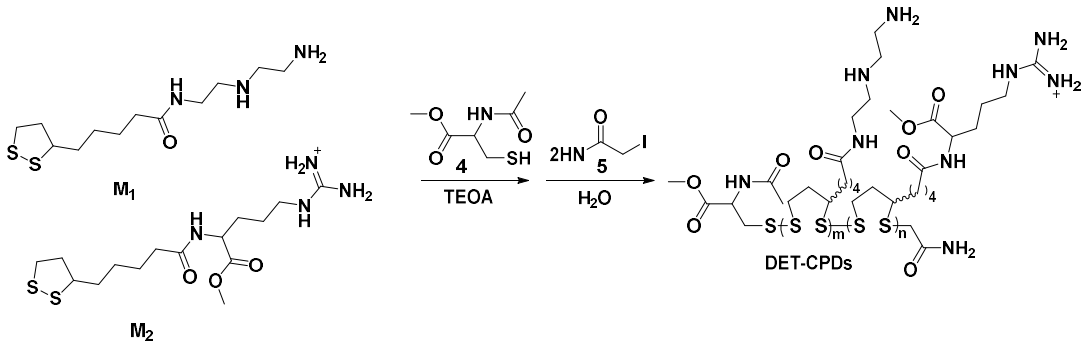


To a solution of initiator **4** (0.03 mM) in 2 ml TEOA buffer (1.0 M, pH = 7) was added in solution of **M1** and **M2** (the ratios range from 1:1, 1:2 to 2:1, 2.4 mM in total) in 10 ml TEOA buffer and then the reaction mixture stirred vigorously for a while in $N_2$ atmosphere. For polymerization, the sample kept at room temperature with vigorous agitation, after 1.5 h, the polymerization mixture was taken and quenched in a solution of terminator **5** (12 mM) in water, and then the mixture was dialyzed in water for 7 days, obtaining the poly(disulfide)s named DET-CPD-1, DET-CPD-2, DET-CPD-3, respectively.

To a solution of initiator **4** (0.03 mM) in 2 ml TEOA buffer (1.0 M, pH = 7) was added in solution of **M1** and **M2** (1:2 in ratio, 2.4 mM in total) in 10 ml TEOA buffer and then the reaction mixture stirred vigorously for a while in $N_2$ atmosphere. For polymerization, the sample kept at room temperature with vigorous agitation, after a fixed period of time (30 min, 1.0 h, 2.0 h, 2.5 h, 3.0 h), 2.4 ml of polymerization mixture was taken and quenched in a solution of terminator **5** (2.4 mM) in water, and then the mixture was dialyzed in water for 7 days, obtaining the poly(disulfide)s named DET-CPD-4, DET-CPD-5, DET-CPD-6, DET-CPD-7, DET-CPD-8, respectively.

To a solution of initiator **4** (0.12 mM) in 2 ml TEOA buffer (1.0 M, pH = 7) was added in solution of **M1** and **M2** (1:2 in ratio, 2.4 mM in total) in 10 ml TEOA buffer and then the reaction mixture stirred vigorously for a while in $N_2$ atmosphere. For polymerization, the sample kept at room temperature with vigorous agitation, after 1.5 h, the polymerization mixture was quenched in a solution of terminator **5** (12 mM) in water, and then the mixture was dialyzed in water for 7 days, obtaining the poly(disulfide) named DET-CPD-9.

To a solution of initiator **4** (0.06 mM) in 2 ml TEOA buffer (1.0 M, pH = 7) was added in solution of **M1** and **M2** (1:2 in ratio, 2.4 mM in total) in 10 ml TEOA buffer and then the reaction mixture stirred vigorously for a while in $N_2$ atmosphere. For polymerization, the sample kept at room temperature with vigorous agitation, after 1.5 h, the polymerization mixture was quenched in a solution of terminator **5** (12 mM) in water, and then the mixture was dialyzed in water for 7 days, obtaining the poly(disulfide) named DET-CPD-10.

To a solution of initiator **4** (0.015 mM) in 2 ml TEOA buffer (1.0 M, pH = 7) was

added in solution of **M1** and **M2** (1:2 in ratio, 2.4 mM in total) in 10 ml TEOA buffer and then the reaction mixture stirred vigorously for a while in $N_2$ atmosphere. For polymerization, the sample kept at room temperature with vigorous agitation, after 1.5 h, the polymerization mixture was quenched in a solution of terminator **5** (12 mM) in water, and then the mixture was dialyzed in water for 7 days, obtaining the poly(disulfide) named DET-CPD-11.

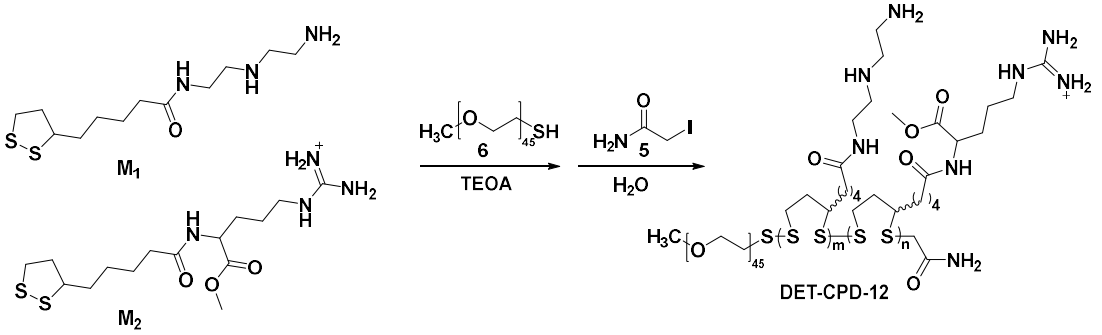


To a solution of initiator **6** (0.03 mM) in 2 ml TEOA buffer (1.0 M, pH = 7) was added in solution of **M1** and **M2** (1:2 in ratio, 2.4 mM in total) in 10 ml TEOA buffer and then the reaction mixture stirred vigorously for a while in $N_2$ atmosphere. For polymerization, the sample kept at room temperature with vigorous agitation, after 1.5 h, the polymerization mixture was taken and quenched in a solution of terminator **5** (12 mM) in water, and then the mixture was dialyzed in water for 7 days, obtaining the poly(disulfide) named DET-CPD-12. $^1$H NMR (400 MHz, $D_2O$) δ 4.29 (s, 9H), 4.06 (s, 2H), 3.64 (s, 27H), 3.59 (s, 190H), 3.26 (s, 18H), 3.10 (s, 54H), 2.79 (s, 78H), 2.21 (s, 68H), 1.55 (s, 196H).

**GPC analysis**

The column of GPC was a Superdex$^{TM}$ 75 10/300 GL (GE, made in USA), and the mobile phase was 30% ACN in 0.1 M acetate buffer (pH = 6.5). The temperature of the column oven was 80 ℃, and 50 μl of the sample was loaded in the column each time and the flow rate of eluent was kept at 0.4 ml/min from 0 to 20 min. The absorbing peak of 214 nm was used to detect the polymerization samples by a Waters 2489 UV/Vis detector, the standard samples were somatostatin (1638 Da), thymosin α1 (3108 Da), recombinant human insulin (5808 Da), ribonuclease A (13700 Da) and β-lactoglobulin (35000 Da).

**Plasmid construction and mRNA in vitro transcription**

Plasmids CMV-Cas9-GFP-U6-sgRNA and CMV-Cas9-GFP-luciferase-U6-sgRNA were constructed using an in-fusion cloning strategy, in which all DNA fragments (Cas9, GFP, luciferase, and U6-sgRNA) amplified by PCR and were ligated to plasmid CMV-Cas9. For CMV-dCas9 plasmid, dCas9-10×GCN4-P2A-SPH-T2A-GFP fragments were amplified from AP111 (Addgene #107307) by PCR and were inserted into backbone plasmid of CMV promoter constructed in our lab previously[2]. For exogenous mCherry activation, a weak promoter miniCMV was ligated to mCherry

fragment, and one dCas9 target sequence (5'-GTCCCCTCCACCCCACAGTG-3') was added upstream of the miniCMV-mCherry plasmid. U6-sgRNA plasmid also contained the same target sequence. *CCNE1* target of Cas9 was designed by CHOPCHOP and was inserted into the plasmids.

For *in vitro* transcription of Cas9 and Cas9-GFP mRNA, the T7-driven plasmids were linearized by NotI and transcribed using HiScribe™ T7 ARCA mRNA Kit (with tailing) (New England Biolabs, MA, USA), following the manufacturer's recommended protocol, and was purified using Monarch RNA Cleanup Kit (New England Biolabs, MA, USA).

**Single-guide RNA (sgRNA) design and synthesis**

sgCCNE1 was designed using the chopchop.cbu.uib.no platform, then prepared using the HiScribe™ T7 Quick High Yield RNA Synthesis Kit (New England Biolabs, MA, USA). The corresponding sgRNA sequence targeting CCNE1 was listed in **Table S2**.

**Cell culture and transfection**

293T, HeLa, HepG2, AML-12, HSCs, Hepa1-6 cells were cultured in Dulbecco's Eagle Medium with high glucose and A549 cells were cultured in RPMI 1640 with high glucose, supplemented with 10% fetal bovine serum, and culturing at 37 ℃ with 5% $CO_2$. The cells were cultured in 48-well plates for 24 h before gene transfection for 6 h in serum-free medium, following by the incubation of polyplexes (0.4 μg plasmid was complexed with different amounts of polymers (2 μl, 3 μg to 16 μl, 24 μg)) dissolved in 250 μl fresh DMEM. The method of mRNA transfection was same as that of pDNA transfection. For protein transfection, 0.5 μg protein was complexed with different amounts of polymer, the mixture solution was diluted in 250 μl serum-free media for 4 h, the media was removed and the cells were washed by PBS, and then the fluorescence microscope was used to visualize the transfection results.

**Cell viability assay**

The cells were transfected with different concentrations of nanoparticles and the cell viability was evaluated by MTT assay kit (MultiSciences, Hangzhou). Briefly, 293T, A549, HeLa or HepG2 cells were seeded in 96-well plates overnight. Then, different concentrations of complexes were transfected in 100 μl DMEM with 10% FBS. After incubation for 48 h, the media was replaced by 100 μl PBS buffer containing 10 μl of MTT solution in each well for 1 h. The absorption of each well at 450 nm was tested by a microplate reader (Thermo Fisher, Germany) to calculate the OD values. The cell viability was determined by the formula: $(OD_{experiment} - OD_{blank}) / (OD_{control} - OD_{blank}) \times 100\%$. $OD_{experiment}$ is the absorbance of the cells treated with various complexes, and $OD_{blank}$ is the absorbance of medium blanks. $OD_{control}$ is the absorbance of the cells without any treatment. In order to investigate the cell viability after BSO treatment, cells were pretreated with BSO (500 μM) for 18 h before adding the complexes solution. The other procedures were the same as the cell viability assay in various points in time.

**Characterization**

TEM image of DET-CPD-12 polyplexes were performed on a transmission electron microscope (HT7700, Hitachi, Japan). Size and zeta potentials of the polyplexes were characterized by DLS at 25 ℃ (Nano ZS90, Malvern Panalytical, UK).

**Gel retardation assay**

The ability of the polymer to condense plasmid DNA was evaluated through gel electrophoresis. Polymer mixed with CMV-Cas9-GFP-luciferase plasmid at different N/P ratios were incubated for 30 min at room temperature, and the mixture was analyzed in 2% agarose gels made from TAE buffer (40 mM Trisacetate, 1 mM EDTA). The gel electrophoresis was carried out at 120 v for 40 min. The procedure of mRNA gel retardation assay was same as the DNA. SDS-PAGE assay was used to evaluate the ability of polymer to complex with Cas9 protein.

***In vitro* release of Cas9 biomacromolecules**

The plasmid or mRNA was mixed with DET-CPD-12 and incubated for 30 min, and the solution mixture was centrifuged (4 min, 12000 rpm) and the supernatant was discarded. The rest of mixture was treated with 10 mM GSH overnight, and then the solution was centrifuged (4 min, 12000 rpm) again. The supernatant was measure for absorbance at 260 nm by a microplate reader (Thermo scientific, Multiskan GO 1050). The release of Cas9 RNP assay was carried out in the same procedure as above, and the released Cas9 RNP was quantified with a BCA kit following the manufacturer's protocol.

**Cellular uptake of CMV-Cas9-GFP-Luciferase plasmid/DET-CPD-12 complexes**

CMV-Cas9-GFP-luciferase plasmid was labeled by rhodamine in red or YOYO-1 in green, and DET-CPD-12 was labeled by FITC in green. For cell organelles, LysoTracker was used to stain lysosomes in red or green, and Hoechst was used to label the nuclear in blue. 293T cells were used to explore the cellular uptake of polyplexes. $10^6$ cells were seeded in cell culture dishes, and the proper amounts of DET-CPD-12/plasmid complexes were added in 1 ml of serum-free culture medium. After the transfection was carried out for 4 h, serum-free culture medium was replaced with fresh DMEM with 10% FBS. The image was visualized by confocal laser scanning microscopy (CLSM, LSM880) at 0.5 h, 3 h and 6 h, respectively. For quantitative analysis of the co-localization between CMV-Cas9-GFP-luciferase plasmid/DET-CPD-12 complexes and LysoTracker Red in 293T cells, Manders' co-localization coefficients between the fluorescence signals of YOYO-1 or FITC labeled nanoparticles and LysoTracker Red were calculated using ImageJ (ImageJ bundled with 64-bit Java 1.8.0_112, https://imagej.nih.gov/ij) with the JACoP co-localization plugin module. The Manders' coefficients M1 was calculated as follow [3]:

$$\mathrm{M1} = \frac{\sum G_{i,co-local}}{\sum G_i} \quad (1)$$

$$G_{i,co-locca} = G_i \; if \; G_i > T_1 \; and \; R_i > T_2 \quad (2)$$

$$G_i = Green \; fluorescence \; intensity \quad if \; G_i > T_1 \quad (3)$$

where subscript i represents the ith pixel in the fluorescence image, G represents green fluorescence intensity, R represents red fluorescence intensity, $T_1$ represents the threshold for the green channel and $T_2$ represents the threshold for the red channel. The two fluorescence intensities and thresholds were determined by the built-in algorithm of the JACoP co-localization plugin module of ImageJ for both the green and red channels.

**T7 Endonuclease 1 (T7E1) assays and deep-sequencing analysis**

The T7E1 assay was used to assess the indel frequency of target genomic loci. After transfection, the cells were collected to extract the DNA using a DNeasy Blood & Tissue Kit (Vazyme, China). Each specific target genomic locus was amplified by PCR (the detailed sequence of the primers can be found in **Table S3**, using a QIA quick PCR Purification Kit (Vazyme, China). Afterwards, a total of 200 ng of PCR products was used to perform T7E1 assay following the recommended protocol. The digested PCR products were analyzed by 2% agarose gels. The disrupted lanes were imaged by a gel documentation system (c150, Azure Biosystems, USA). The Image J was used to quantify the gray level of digested bands and undigested bands. Indel percentage analysis was calculated with the following formula: $[1-(1-\text{fraction cleaved})^{1/2}] \times 100\%$, where fraction cleaved = the sum of each digested band intensity / (the sum of each digested band intensity + undigested band intensity). For the analysis of genome disruption in the edited tissue, the transfected tissues were first homogenized, and were further analyzed according to the above protocols. At the same time, these PCR products were quantified using deep-sequencing assay.

**Off-target analysis**

The most potential off-target sites that are corresponding to the on-target genome locus (*CCNE1*) were identified with an online tool, Cas-OFFinder (http://www.rgenome.net/cas-offinder/). All the off-target sites and primers for PCR amplification were listed in **Table S4** and **Table S5**. Off-target analysis procedure was similar to on-target examination through Sanger sequencing. The sequence of analyzed off-target sites were also evaluated by deep-sequencing after the nanoparticle transfection. A library of genomic DNA pooled from the sample in triplicate was subjected to deep-sequencing analysis. Deep-sequencing analysis of *CCNE1* off-target sites in **Table S6**. The detailed procedures for deep-sequencing were described previously[2].

**Establishment the fulminant hepatic failure (FHF) mice**

Female BALB/c nude mice (6-8 weeks old) were fed in the Laboratory in Animals Centre, Zhejiang University, and were supplied with sterilized air, water, and food. All animal treatments or procedures were approved by the Laboratory Animal Welfare and

Ethics Committee of Zhejiang University (Approval No.: 18286). Acetaminophen (APAP) was dissolved in PBS at 55 ℃, and then the solution was cooled down to 37 ℃. The mice were subjected by the intraperitoneal injection of APAP at the dose of 250 mg/kg after being fasted overnight. The mice were treated with nanocomplexes 2 days prior to the administration of APAP. For treatment, the mice were given a dose of 30 μg of plasmid, 30 μg of mRNA or 50 μg of protein, respectively.

**Hemolysis assay**

The blood compatibilities of DET-CPD-12/CMV-Cas9-GFP-Luciferase plasmid nanoparticles were evaluated by a hemolysis test on the Murine erythrocytes of rat. Blood was obtained from male SD rats (6-12 months). At first, the anticoagulated red blood cells were isolated by centrifugation at 2000 rpm for 10 min and washed with PBS solution for 5 times, and resuspended in 20 mM HEPES (pH 7.4) or 20 mM MES (pH 5.5) containing 150 mM NaCl for the pH adjustment. The DET-CPD-12/CMV-Cas9-GFP-Luciferase plasmid nanoparticles (100 μg/ml) in the same buffer were added to the erythrocyte solutions (1 ml) and incubated at 37 °C in Eppendorf tube (1.5 ml) for 3 h. The liberated hemoglobin was determined after centrifugation (2000 rpm for 5 min) by the absorbance of the supernatant solution of test ($A_{test}$), positive control ($A_{pos}$), and negative control ($A_{neg}$) at 541 nm were measured by UV−Vis spectrophotometer. Each set of experiments was carried out three times. The value for 100% hemolysis was set at 0.2 wt% Tween 20 as the positive control ($A_{pos}$), and the PBS as the negative control ($A_{neg,}$ 0%).

The hemolysis (%) = $[(A_{test} - A_{neg}) / (A_{pos} - A_{neg})] \times 100\%$.

**Statistical analysis**

All statistical analyses were performed using GraphPad Prism version 8 software (GraphPad Software Inc.). All results were expressed as means ± SD. Biological replicates were used in all experiments unless otherwise stated. The statistical significance was analyzed using Students' t-test and analysis of variance (ANOVA). One-way ANOVA with a Tukey's post-hoc test was used when more than two groups were compared. Survival benefit was determined using a log-rank test. $P < 0.05$ was considered significant. No Significance (*N.S.*), $P > 0.05$; $*P < 0.05$, $**P < 0.01$, $***P < 0.001$ and $****P < 0.001$.

**References**

[1] E. K. Bang, G. Gasparini, G. Moinard, A. Roux, N. Sakai, S. Matile, *J. Am. Chem. Soc*. **2013**, *135*, 2088-2091.

[2] X, Chen, Y. Chen, H. Xin, T. Wan, Y. Ping, *Proc. Natl. Acad. Sci.* **2020***,117*. 2395-2405.

[3] J. Xu, Y. Liu, Y. Li, H. Wang, S. Stewart, K. V. Jeught, P. Agarwal, Y. Zhang, S. Liu, G. Zhao, J. Wan, X. Lu, X. He, *Nat. Nanothechol.* **2019**, *14*, 388-397.

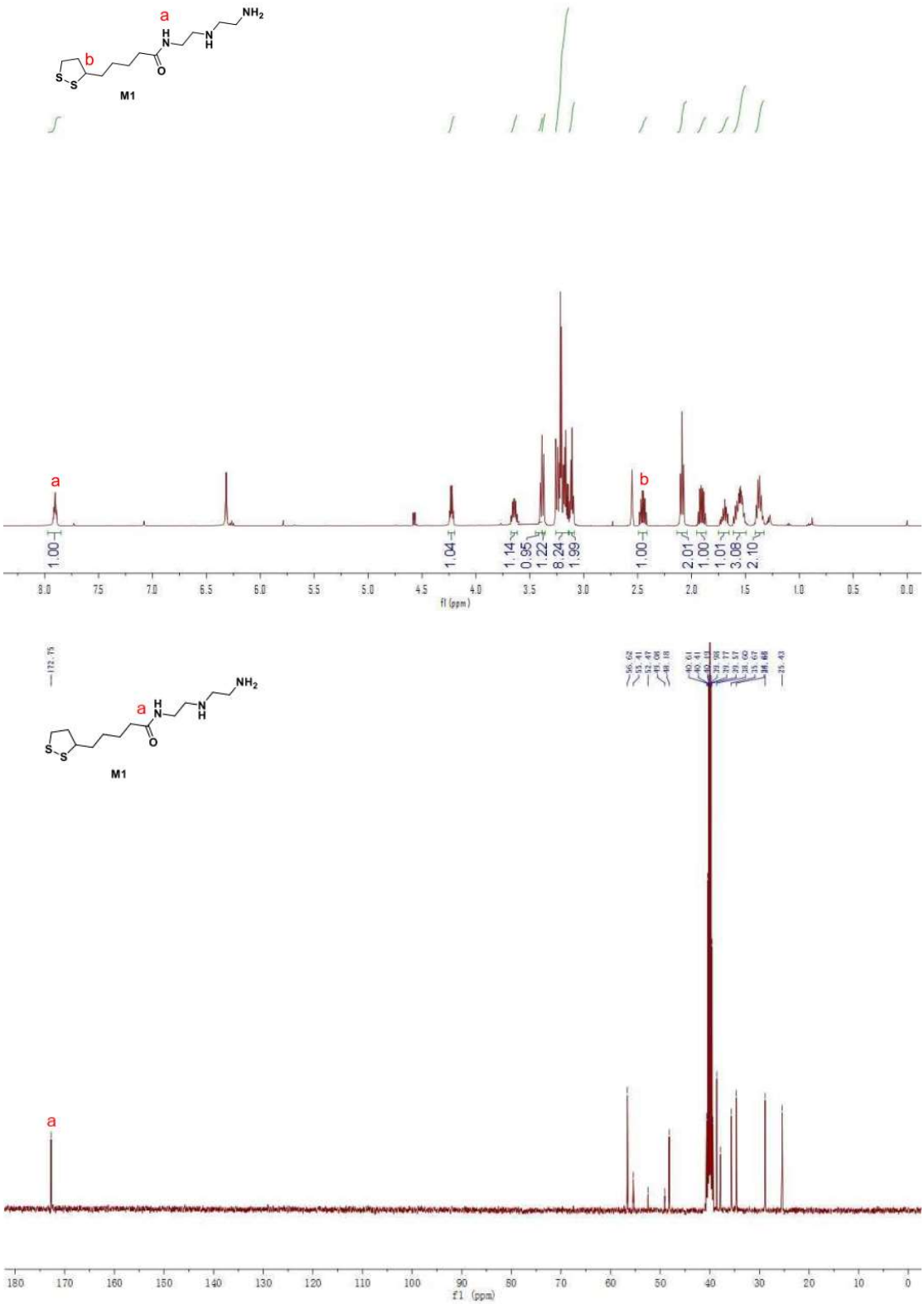


**Figure S1.** $^{1}H$ NMR, and $^{13}C$ NMR spectra of M1 in DMSO-$d_6$.

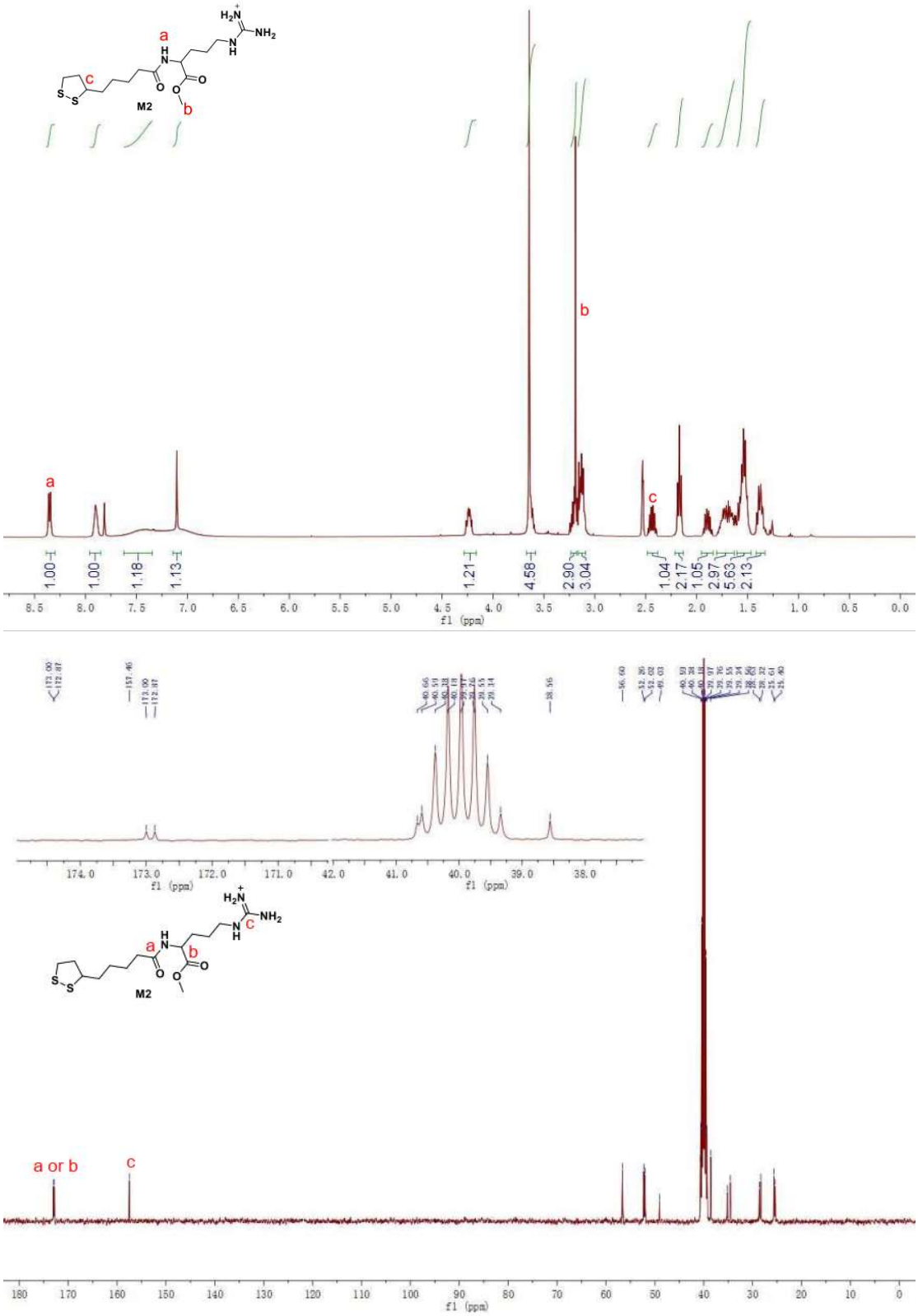


**Figure S2.** $^{1}$H NMR, and $^{13}$C NMR spectra of M2 in DMSO-$d_6$.

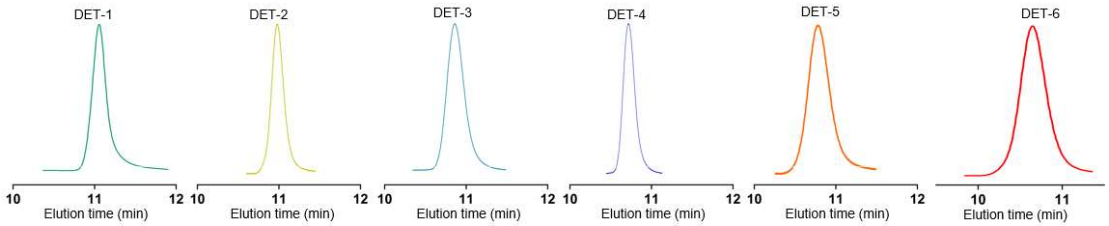


**Figure S3.** The GPC profiles of DETs.

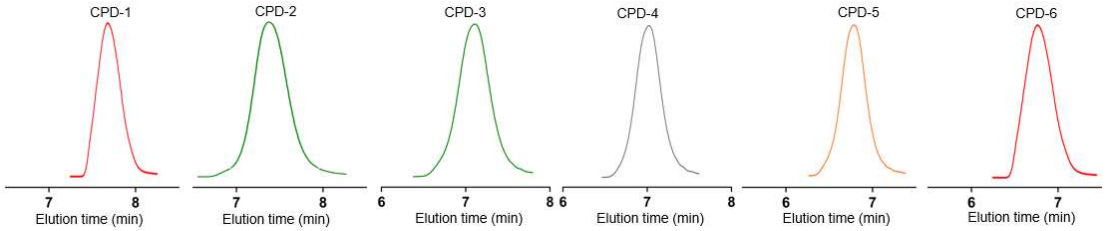


**Figure S4.** The GPC profiles of CPDs.

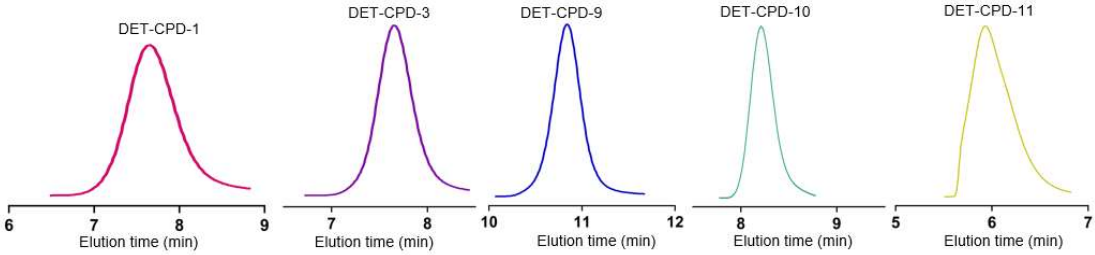


**Figure S5.** The GPC profiles of DET-CPDs.

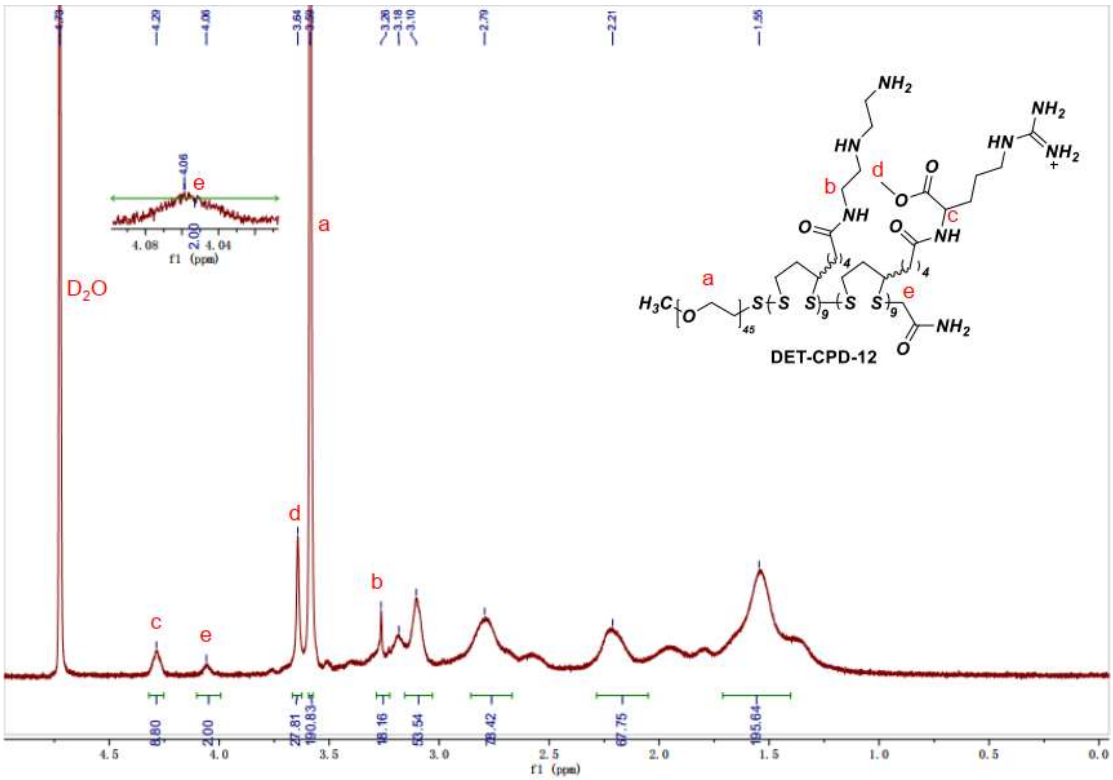


**Figure S6.** $^{1}$H NMR spectra of DET-CPD-12 in $D_2O$.

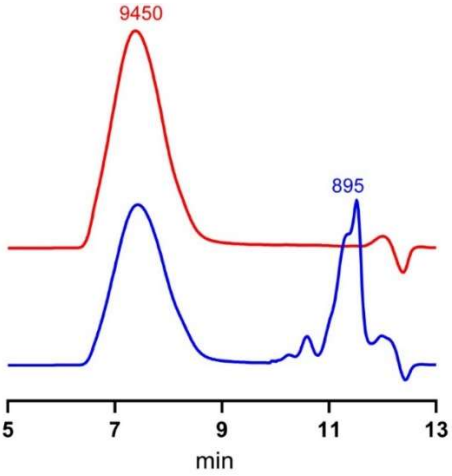


**Figure S7.** GPC analysis of DET-CPD-12 and the degradation of DET-CPD-12 in the presence of 10 μM GSH after the incubation for 24 h.

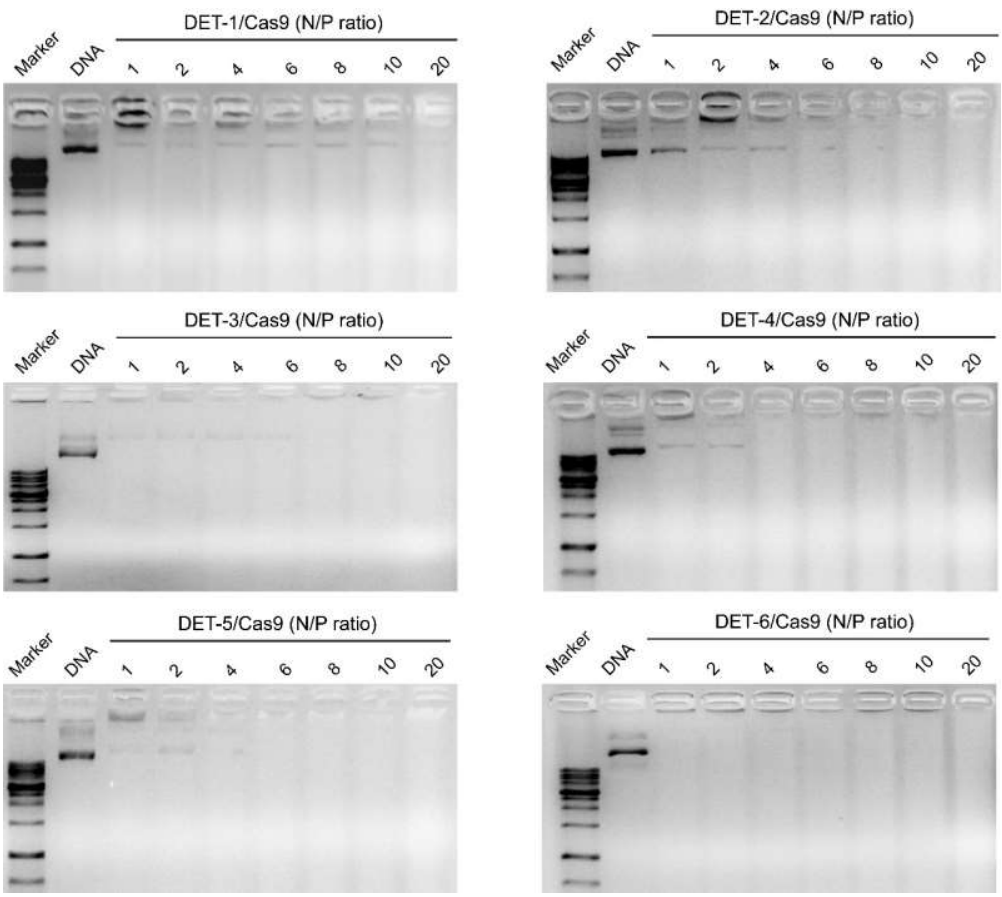


**Figure S8.** Agarose gel electrophoresis assay of CMV-Cas9-GFP-luciferase plasmid complexed with DETs at different N/P ratios. Lane 1 represents the DNA marker, lane 2 represents the naked DNA, and lane 3-9 represent DETs/CMV-Cas9-GFP-luciferase complexes at N/P ratios range from 1:1, 2:1, 4:1, 6:1, 8:1, 10:1 to 20:1, respectively.

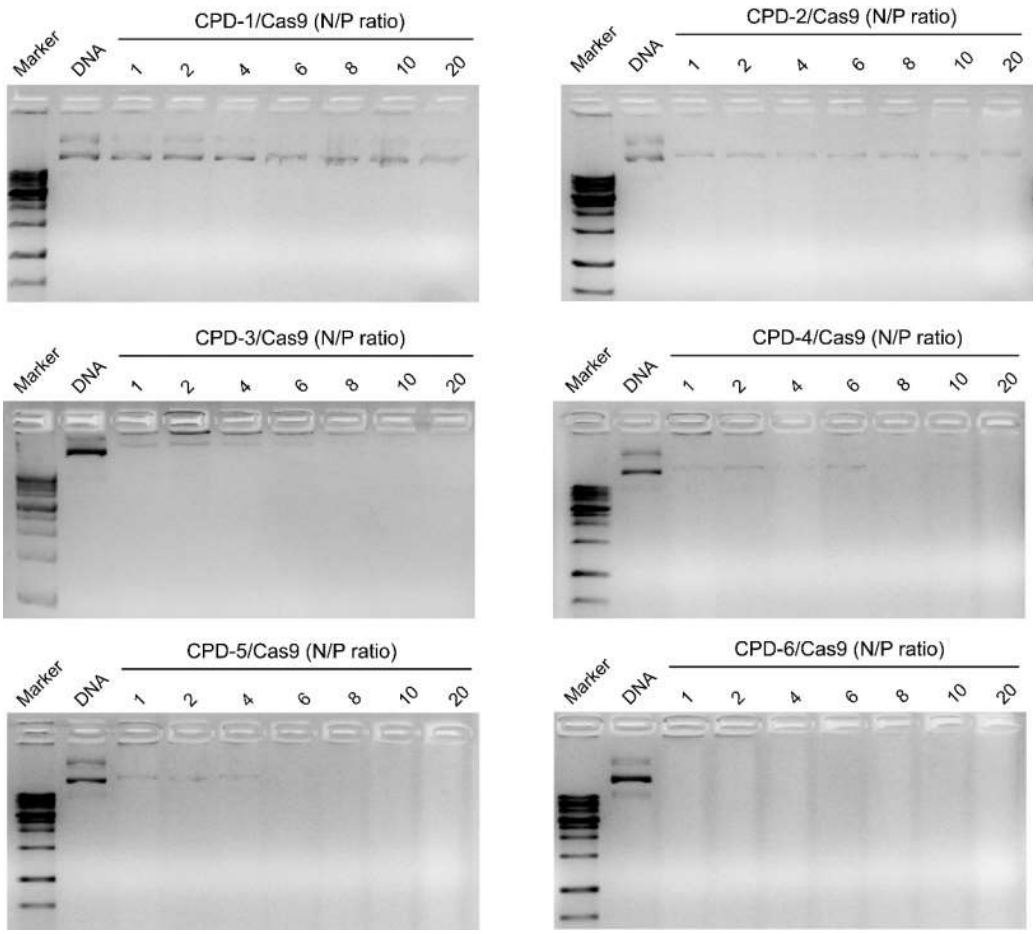


**Figure S9.** Agarose gel electrophoresis assay of CMV-Cas9-GFP-luciferase plasmid complexed with CPDs at different N/P ratios. Lane 1 represents the DNA marker, lane 2 represents the naked DNA, and lane 3-9 represent CPDs/CMV-Cas9-GFP-luciferase plasmid complexes at N/P ratios range from 1:1, 2:1, 4:1, 6:1, 8:1, 10:1 to 20:1, respectively.

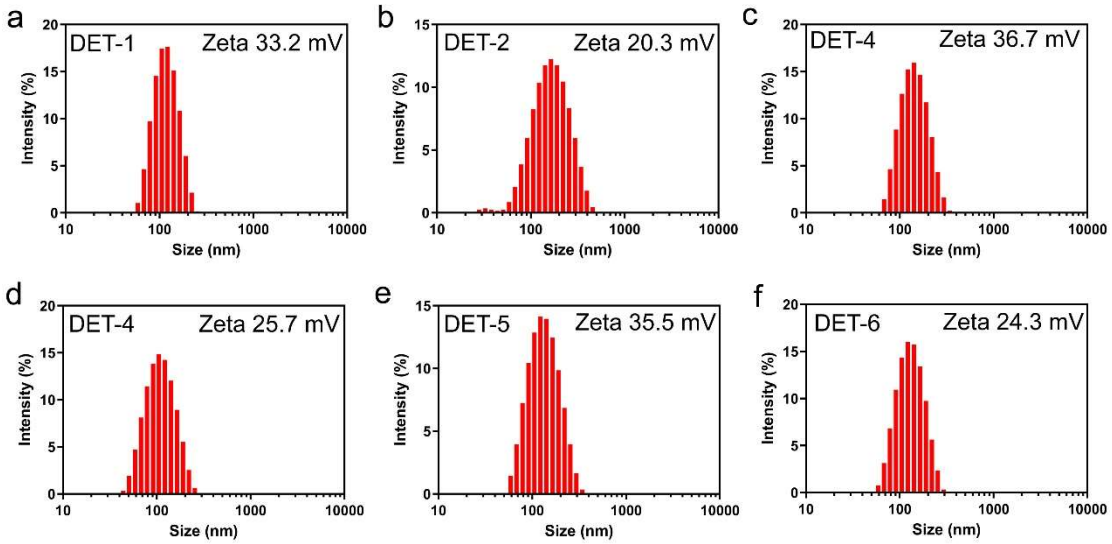


**Figure S10.** Hydrodynamic size and zeta potential of the DETs/CMV-Cas9-GFP-luciferase complexes at N/P ratio of 5 measured by dynamic light scatting. All the samples were conducted at 25 ℃.

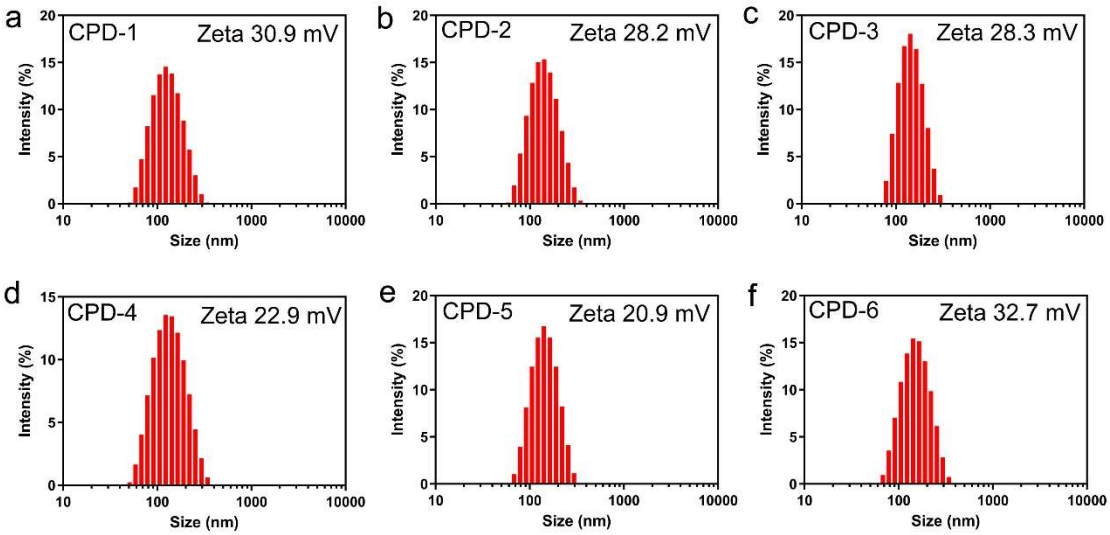


**Figure S11.** Hydrodynamic size and zeta potential of the CPDs/CMV-Cas9-GFP-luciferase complexes at N/P ratio of 5 measured by dynamic light scatting. All the samples were conducted at 25 ℃.

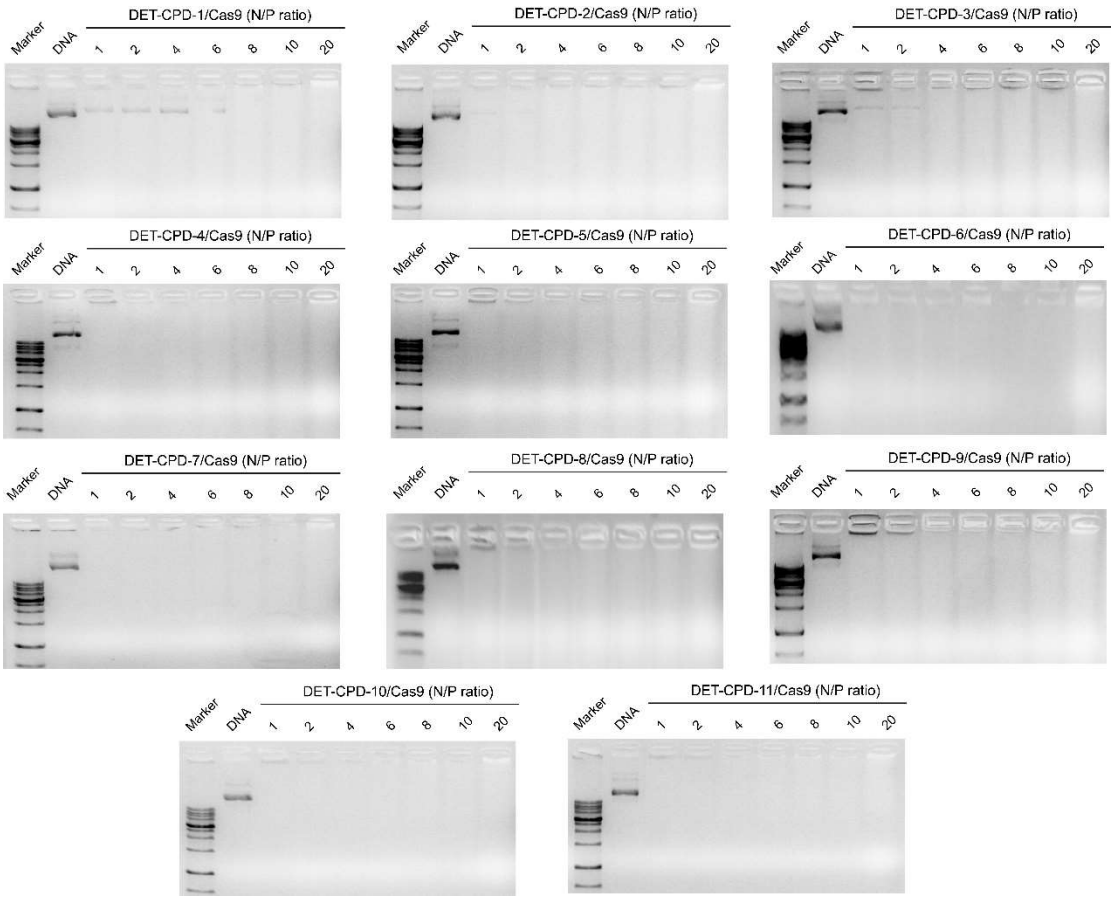


**Figure S12.** Agarose gel electrophoresis assay of CMV-Cas9-GFP-luciferase plasmid complexed with DET-CPDs at different N/P ratios. Lane 1 represents the DNA marker, lane 2 represents the naked DNA, and lane 3-9 represent DET-CPDs/CMV-Cas9-GFP-luciferase plasmid complexes at N/P ratios range from 1:1, 2:1, 4:1, 6:1, 8:1, 10:1 to 20:1, respectively.

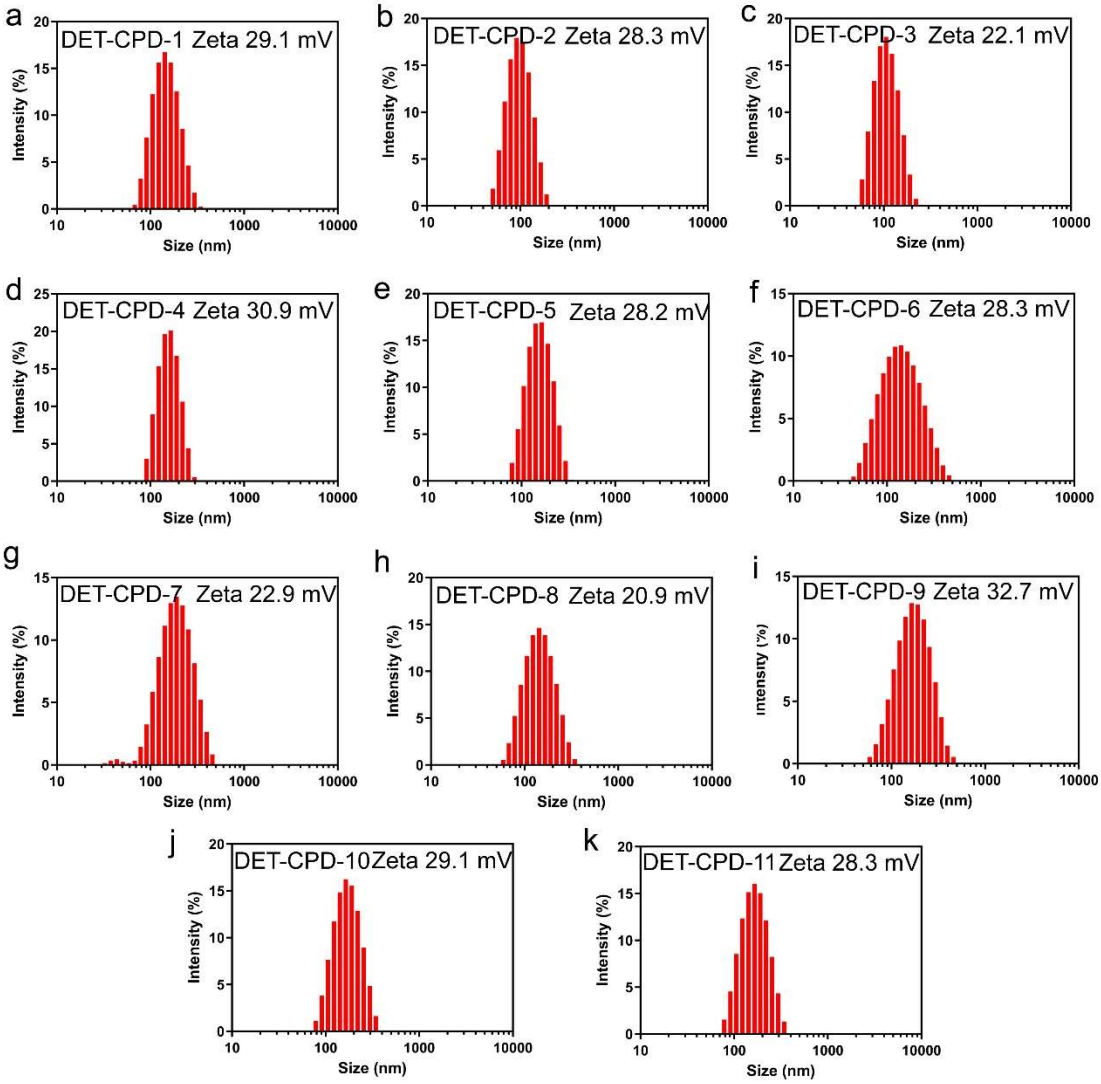


**Figure S13.** Hydrodynamic size and zeta potential of DET-CPDs/CMV-Cas9-GFP-luciferase complexes at N/P ratio of 5 measured by dynamic light scatting. All the samples were conducted at 25 ℃.

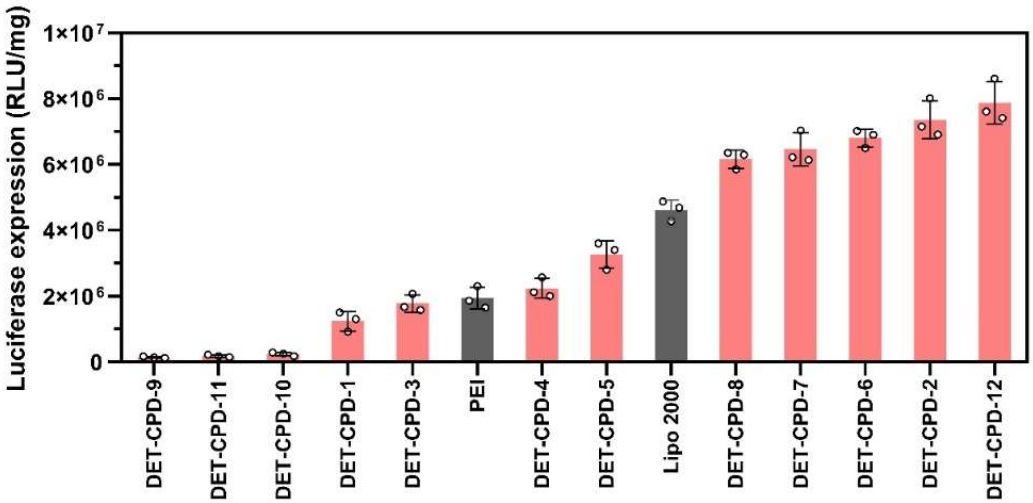


**Figure S14.** CMV-Cas9-GFP-Luci plasmid transfected by DET-CPDs in 293T cells. Commercially available Lipo 2000 and PEI 25K were used as the positive controls. Data represent mean ± S. D. ($n$ = 3).

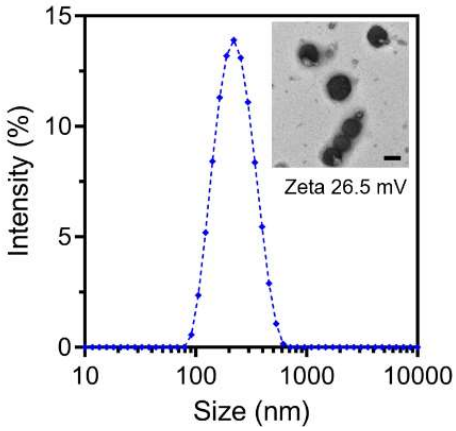


**Figure S15.** The Particle size and zeta potential of DET-CPD-12/Cas9 RNP complexes, and the inset is the TEM image of the nanoparticles. The scale bar represents 200 nm.

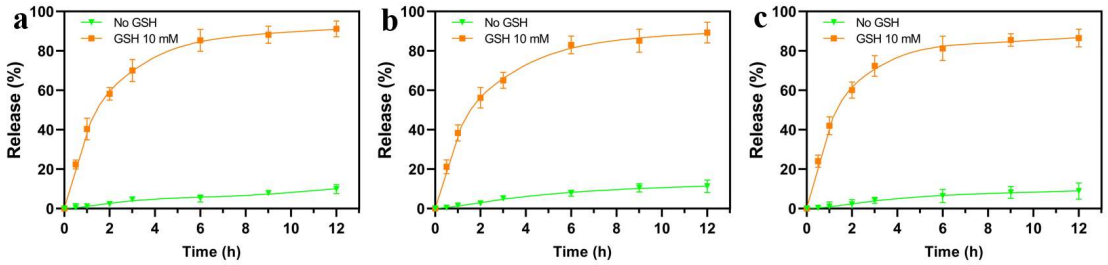


**Figure S16.** The vitro biomacromolecule release from (a) DET-CPD-12/Cas9 DNA complexes, (b) DET-CPD-12/Cas9 mRNA complexes, and (c) DET-CPD-12/Cas9 protein complexes in addition of GSH (10 mM) or in PBS buffer for 12 h.

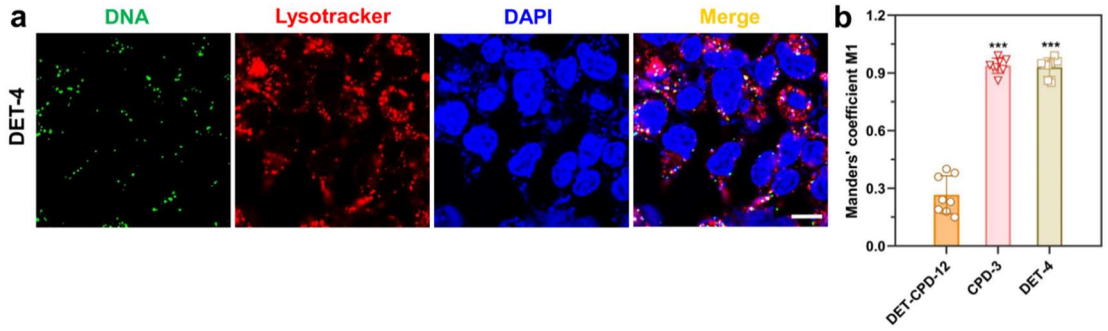


**Figure S17.** Cellular uptake and endosomal escape of DET-4/Cas9 plasmid nanocomplexes in 293T cells, as evaluated by confocal laser scanning microscopy. (a) Plasmid DNA was labeled by YOYO-1 in green, the nucleus was labeled by Hoechst in blue, and endosome was labeled by Lysotracker in red. (b) Quantitative analysis of co-localization of YOYO-1 labeled plasmid with endo/lysosomes labeled with LysoTracker red. Manders' coefficient M1 denotes the fraction of YOYO-1 labeled plasmid in green overlapping with LysoTracker red. The coefficients are close to 1 if they are highly co-localized (n = 8 images from three independent experiments). The scale bar represents 20 μm, one-way ANOVA with a Tukey post-hoc test, ***$P < 0.001$.

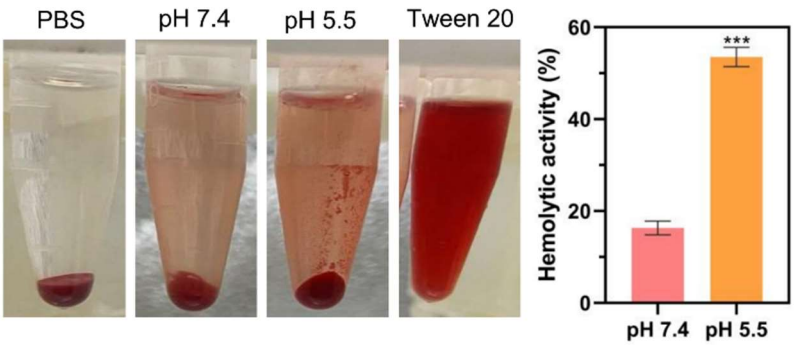


**Figure S18.** The hemolytic activity of DET-CPD-12/Cas9 plasmid nanoparticles against murine erythrocytes. Hemolytic activity of DET-CPD-12/Cas9 plasmid incubated with erythrocyte were conducted at pH 7.4 or pH 5.5 after 3 h of incubation at 37 °C. The PBS was used as the negative control (0% for hemolytic activity), and 100% hemolytic activity was defined by erythrocyte hemolysis treated with 0.2% Tween 20, which was used as the positive control. The error bar represents the standard error (mean ± S.D., $n = 3$, one-way ANOVA with a Tukey post-hoc test, $^{***}P < 0.001$).

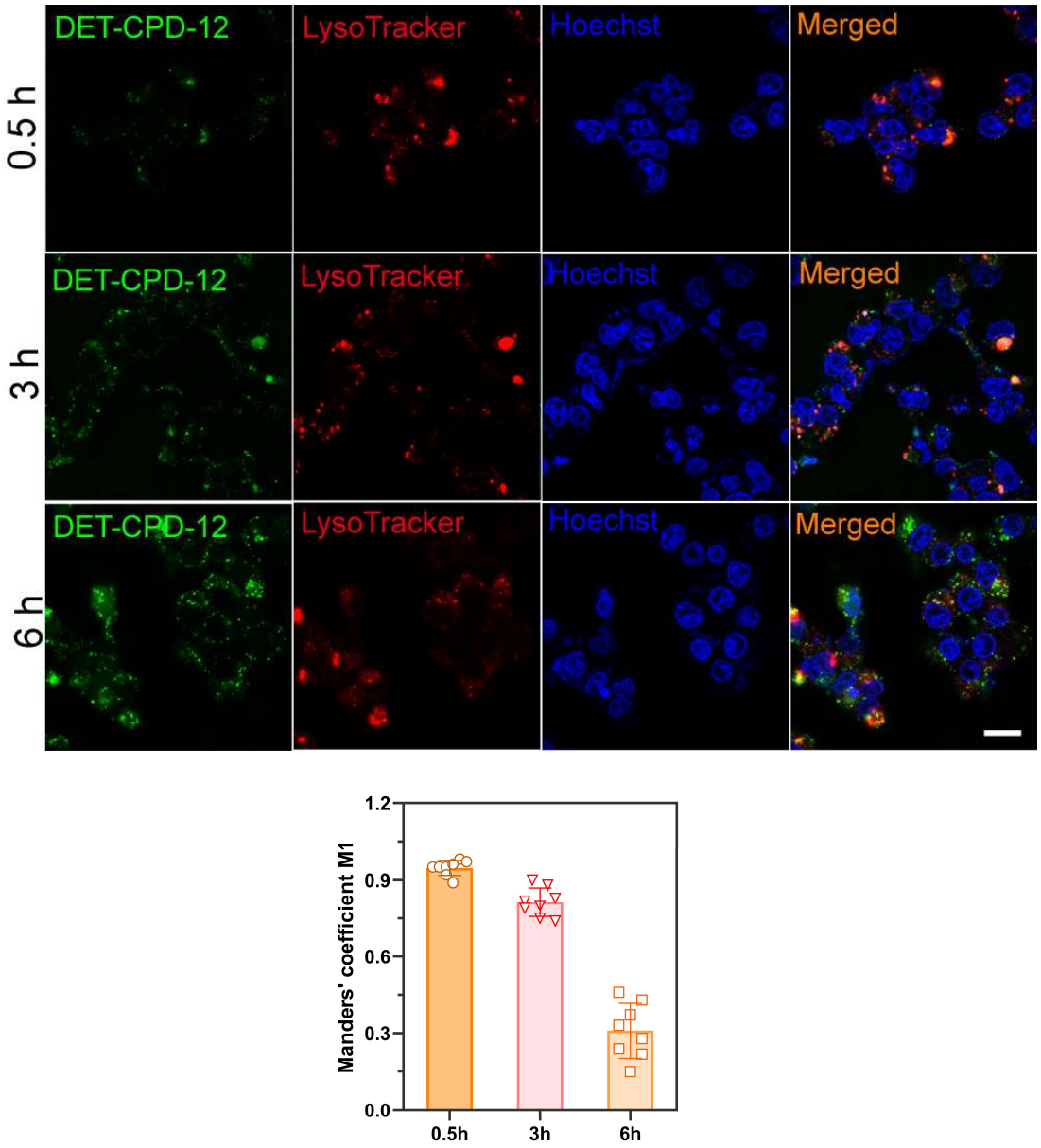


**Figure S19.** Cellular uptake and endosomal escape experiments. CLSM images of the cellular uptake and escape of DET-CPD-12/Cas9 DNA nanocomplexes from endosome in 293T cells after transfection for 0.5 h, 3 h or 6 h, respectively. The DET-CPD-12 was labeled by FITC in green, LysoTracker labeled the lysosome in red, and the nucleus was labeled by Hoechst in blue. Quantitative analysis of co-localization of FITC labeled DET-CPD-12 with endo/lysosomes labelled with LysoTracker red. Manders' coefficient M1 denotes the fraction of FITC labeled DET-CPD-12 in green overlapping with LysoTracker red. The coefficients are close to 1 if they are highly co-localized (n = 8 images from three independent experiments). The scale bar represents 20 μm.

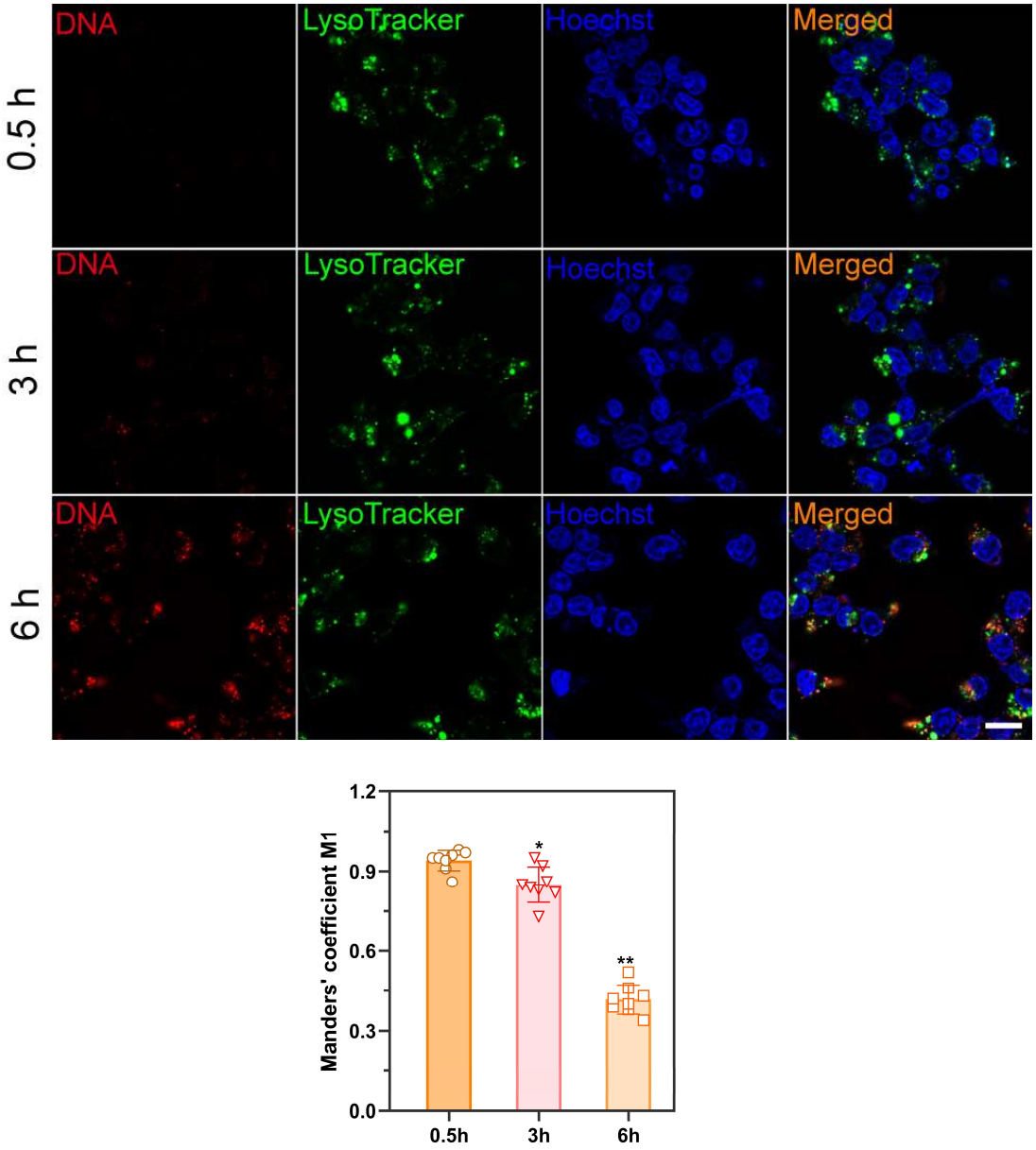


**Figure S20.** Cellular uptake and endosomal escape experiments. CLSM images of the cellular uptake and escape of the DET-CPD-12/Cas9 plasmid nanocomplexes from endosomes in 293T cells after the transfection for 0.5 h, 3 h or 6 h, respectively. The plasmid was labeled by rhodamine in red, LysoTracker labeled the lysosome in green, and the nucleus was labeled by Hoechst in blue. Quantitative analysis of co-localization of rhodamine labeled plasmid with endo/lysosomes labelled with LysoTracker green. Manders' coefficient M1 denotes the fraction of rhodamine labeled plasmid in red overlapping with LysoTracker green. The coefficients are close to 1 if they are highly co-localized ($n = 8$ images from three independent experiments). The scale bar represents 20 μm.

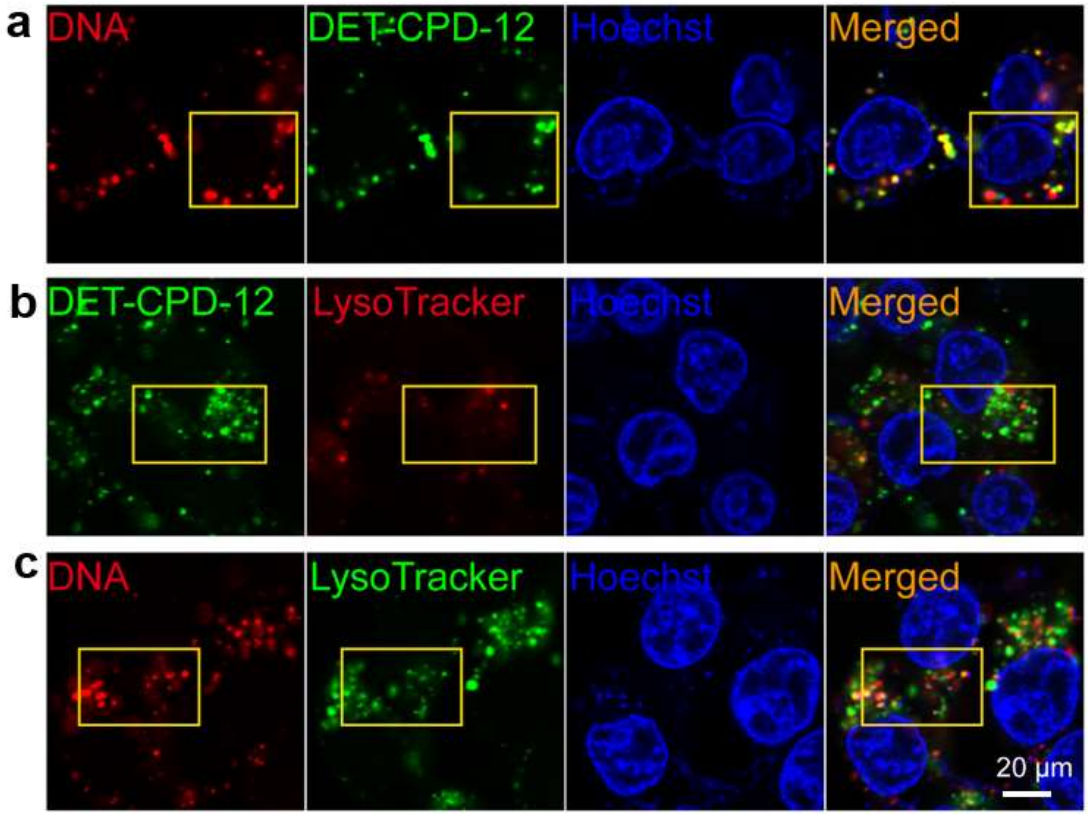


**Figure S21.** Cellular uptake and endosomal escape experiments. CLSM images of the cellular uptake and escape of the DET-CPD-12/Cas9 plasmid nanocomplexes from endosomes in 293T cells after the transfection for 6 h, Plasmid DNA was labeled by rhodamine in red, DET-CPD-12 was labeled by FITC in green, and Lysotracker labeled the lysosome in red or green, and the nucleus was labeled by Hoechst in blue. The scale bar represents 20 μm.

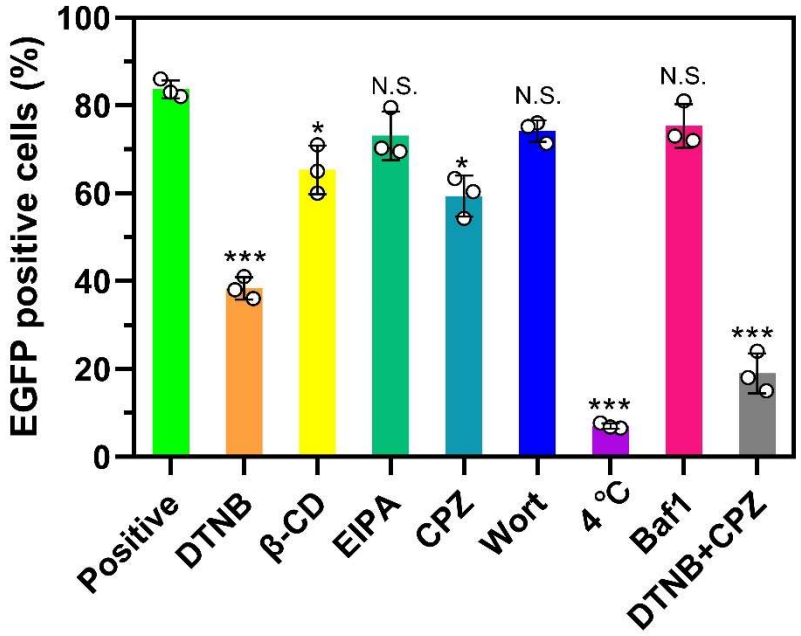


**Figure S22.** Study of endocytosis mechanism. The quantification of GFP expression of CMV-Cas9-GFP-Luci plasmid mediated by DET-CPD-12 in 293T cells treated by endocytosis inhibitors (2 h incubation at 37 ℃), including 5,5'-dithiobis-2-nitrobenzoic acid (DTNB, 2.4 nM), methyl-β-cyclodextrin (β-CD), amiloride (EIPA), chlorpromazine (CPZ), wortmannin (wort), bafilomycin A1 (Baf1). The assays were also conducted at 4 ℃ (no inhibitor) or in the presence of DTNB and CPZ. Positive control was normalized to those of 293T cells treated with DET-CPD-12/CMV-Cas9-GFP-Luci plasmid only (37 ℃, no inhibitor). Flow cytometry analysis of EGFP expression mediated by DET-CPD-12/CMV-Cas9-GFP-Luciferase plasmid nanoparticles treated by endocytosis inhibitors. All of the experimental group were compared with the positive group, respectively. (Error bar represent the standard error (mean ± S.D., $n$ = 3, one-way ANOVA with a Tukey post-hoc test, *N.S., $P > 0.05$, *$P < 0.05$, **$P < 0.01$, ***$P < 0.001$*).

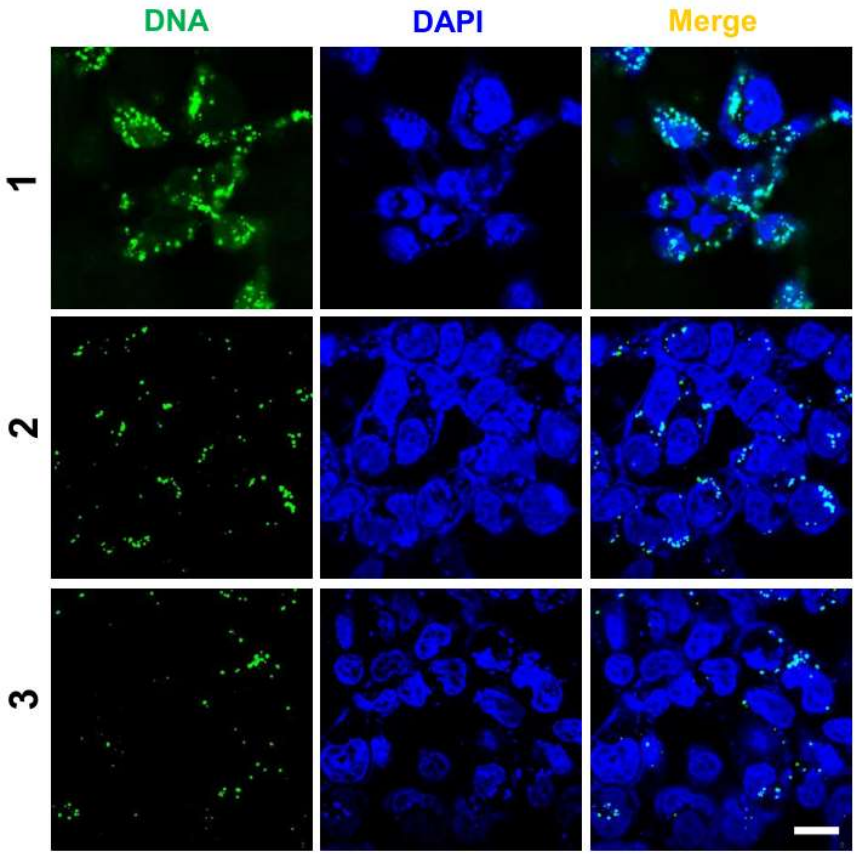


**Figure S23.** Study of uptake mechanism. Cellular uptake of DET-CPD-12/Cas9 plasmid nanocomplexes in 293T cells after transfection for 6 h, as evaluated by confocal laser scanning microscopy. Plasmid DNA was labeled by YOYO-1 in green, the nucleus was labeled by Hoechst in blue. The cells were incubated by different concentrations of DTNB for 2 h (panel 2: 2.4 nM; panel 3: 4.8 nM) before conducting the experiments, the DET-CPD-12/YOYO-1 labeled-Cas9 plasmid without any treatment were used as the positive control (panel 1, 37 ℃). The scale bar represents 20 μm.

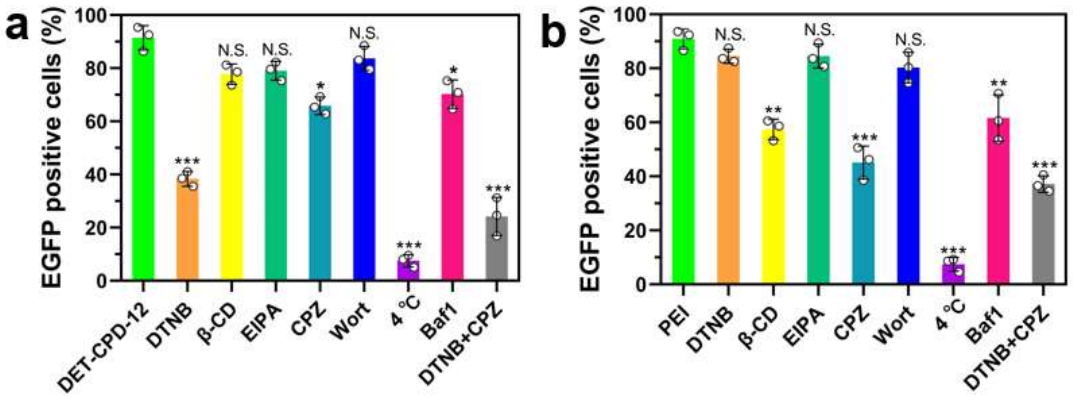


**Figure S24.** Study of endocytosis mechanism. The quantification of GFP expression of CMV-GFP-plasmid mediated by DET-CPD-12 or PEI of 25 kDa in 293T cells treated by endocytosis inhibitors (2 h incubation at 37 ℃), including 5,5'-dithiobis-2-nitrobenzoic acid (DTNB, 2.4 nM), methyl-β-cyclodextrin (β-CD), amiloride (EIPA), chlorpromazine (CPZ), wortmannin (wort), bafilomycin A1 (Baf1). The assays were also conducted at 4 ℃ (no inhibitor) or in the presence of DTNB and CPZ. DET-CPD-12 or PEI data were normalized to those of 293T cells treated with DET-CPD-12/CMV-GFP-plasmid or PEI/CMV-GFP-plasmid only. (a) Flow cytometry analysis of EGFP expression mediated by DET-CPD-12/CMV-GFP-plasmid nanoparticles treated by endocytosis inhibitors. (b) Flow cytometry analysis of EGFP expression mediated by PEI/CMV-GFP-plasmid nanoparticles treated by endocytosis inhibitors. All of the experimental group were compared with the DET-CPD-12 or PEI group, respectively. Error bar represent the standard error (mean ± S.D., $n$ = 3, one-way ANOVA with a Tukey post-hoc test, *N.S., $P > 0.05$, *$P < 0.05$, **$P < 0.01$, ***$P < 0.001$*).

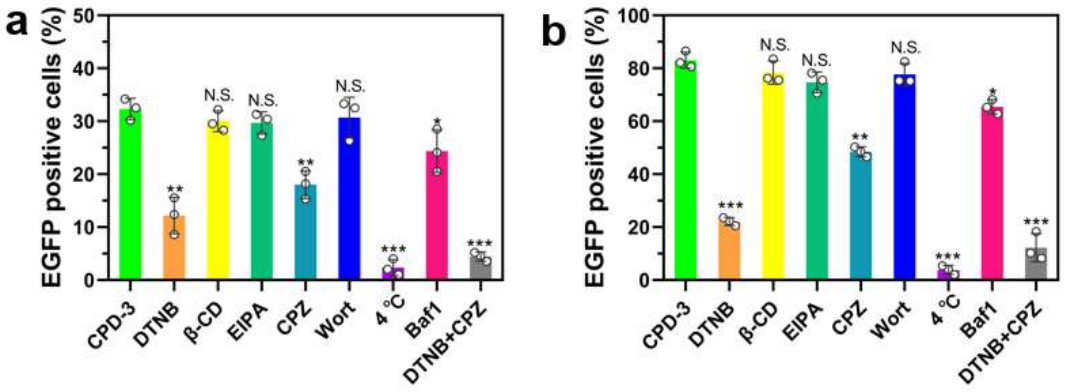


**Figure S25.** Study of endocytosis mechanism. The quantification of GFP expression of CMV-Cas9-GFP-luciferase (a) or CMV-GFP-plasmid (b) mediated by CPD-3 in 293T cells treated by endocytosis inhibitors (2 h incubation at 37 ℃), including 5,5'-dithiobis-2-nitrobenzoic acid (DTNB), methyl-β-cyclodextrin (β-CD), amiloride (EIPA), chlorpromazine (CPZ), wortmannin (wort), bafilomycin A1 (Baf1). The assays were also conducted at 4 ℃ (no inhibitor) or in the presence of DTNB and CPZ. CPD-3 data were normalized to those of 293T cells treated with CPD-3/CMV-Cas9-GFP-luciferase or CPD-3/CMV-GFP-plasmid only. (a) Flow cytometry analysis of EGFP expression mediated by CPD-3/CMV-Cas9-GFP-luciferase nanoparticles treated by endocytosis inhibitors. (b) Flow cytometry analysis of EGFP expression mediated by CPD-3/CMV-GFP-plasmid nanoparticles treated by endocytosis inhibitors. All of the experimental group were compared with the CPD-3 group, respectively. Error bar represent the standard error (mean ± S.D., $n = 3$, one-way ANOVA with a Tukey post-hoc test, *N.S., $P > 0.05$, *$P < 0.05$, **$P < 0.01$, ***$P < 0.001$*).

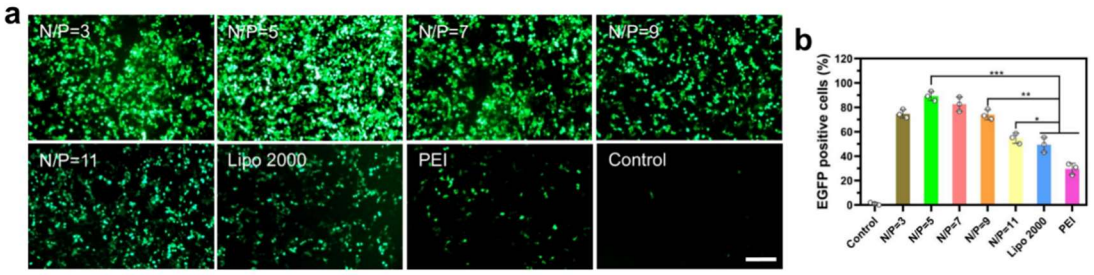


**Figure S26.** Screening the different N/P ratios of DET-CPD-12 mediated the plasmid transfection. (a) GFP expression of DET-CPD-12/CMV-Cas9-GFP-luciferase complexes in 293T cells for 48 h. The N/P ratios for the polymers and plasmid varied from 3 to 11, and the commercially available Lipo 2000 and PEI of 25 kDa were used as the positive controls. (b) Flow cytometry analysis of EGFP expression in cells. The scale bar represents 200 μm. Error bar represents the standard error (mean ± S.D., $n$ = 3, one-way ANOVA with a Tukey post-hoc test, $*P < 0.5$, $**P < 0.01$, $***P < 0.001$).

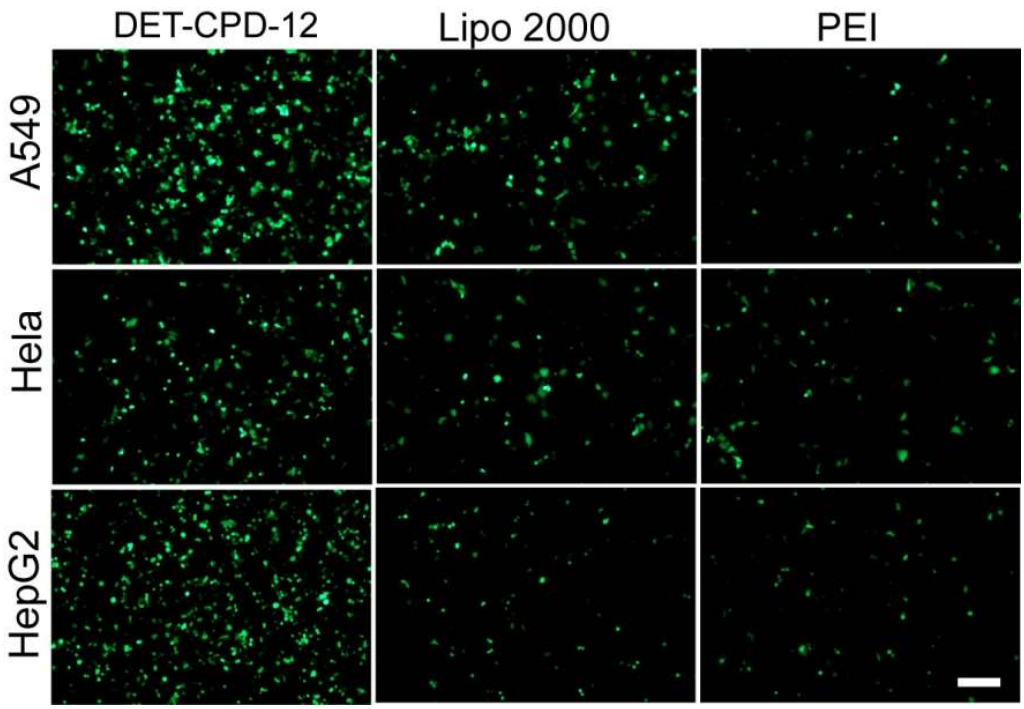


**Figure S27.** The fluorescent image of GFP expression of DET-CPD-12/CMV-Cas9-GFP-luciferase complexes in A549 cells, HeLa cells and HepG2 cells for 48 h, respectively. Lipo 2000 and PEI of 25 kDa were used as the positive controls. The scale bar represents 200 μm.

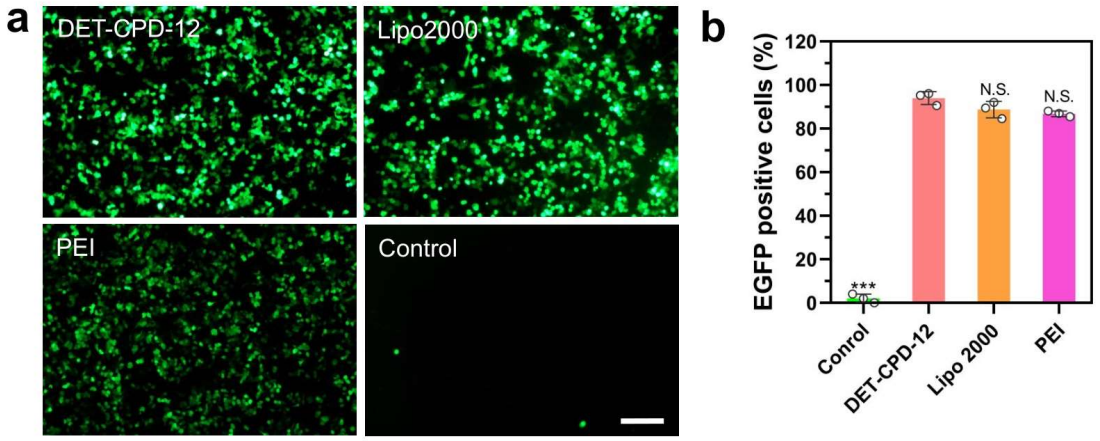


**Figure S28.** DET-CPD-12 mediated the GFP plasmid transfection. (a) EGFP expression of DET-CPD-12/CMV-GFP complexes in 293T cells for 48 h, using Lipo 2000 and PEI of 25 kDa as the positive controls. (b) Flow cytometry analysis of EGFP expression in the transfected cells. The scale bar represents 200 μm. Error bar represent the standard error (mean ± S.D., $n = 3$, one-way ANOVA with a Tukey post-hoc test, *N.S., $P > 0.05$. ***$P < 0.001$*).

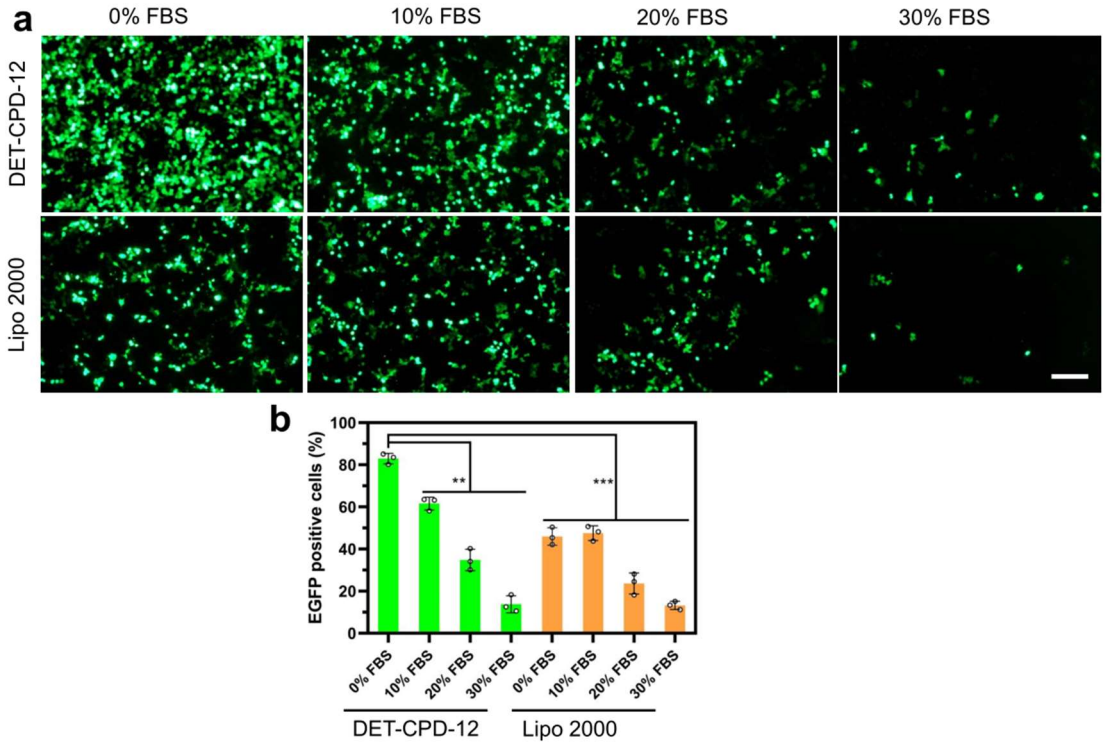


**Figure S29.** The transfection of Cas9 plasmid with a GFP tag mediated by DET-CPD-12 in the serum-containing medium. (a) GFP expression after the transfection in 293T cells containing 0%, 10%, 20%, 30% serum was visualized. Lipofectamine 2000 (Lipo 2000) was used as the positive control. (b) Flow cytometry analysis of EGFP expression. The scale bar represents 200 μm. The error bar represents the standard error (mean ± S.D., $n = 3$, one-way ANOVA with a Tukey post-hoc test, **$P < 0.01$, ***$P < 0.001$*).

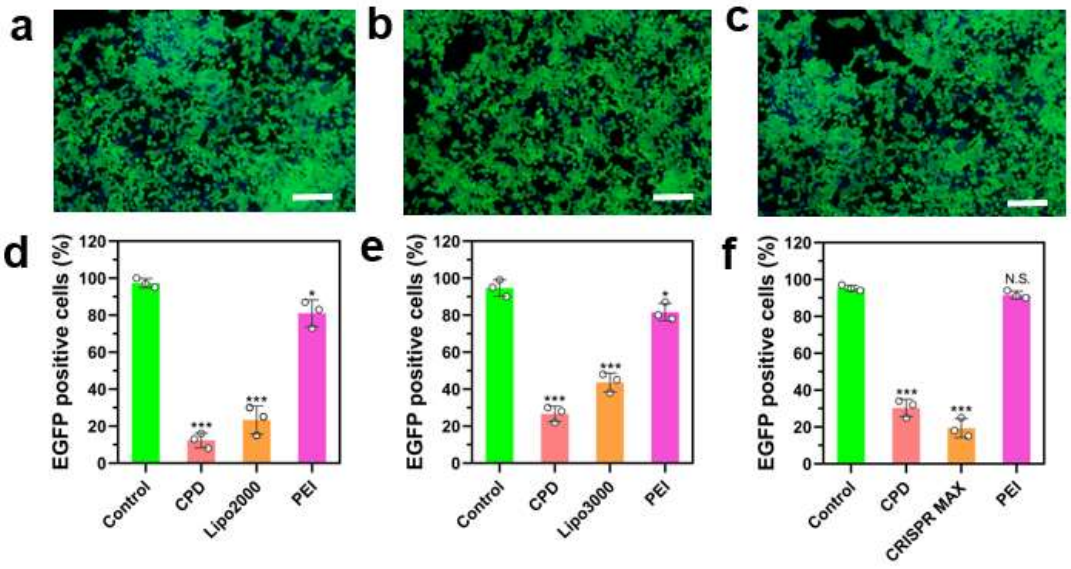


**Figure S30.** EGFP gene disruption assays. Image (a), (b), and (c) represent the negative control (cells without any treatment) for DET-CPD-12/plasmid (corresponding to Figure 4g), DET-CPD-12/Cas9-mRNA (corresponding to Figure 5b), and DET-CPD-12/Cas9 RNP (corresponding to Figure 5f) respectively. Flow cytometry analysis of 293T-EGFP cells treated by DET-CPD-12/Cas9 plasmid complexes (d), DET-CPD-12/CMV-Cas9-mRNA complexes (e), and DET-CPD-12/Cas9 RNP nanocomplexes (f). The scale bar represents 200 μm. The error bar represents the standard error (mean ± S.D., $n$ = 3, one-way ANOVA with a Tukey post-hoc test, *N.S., $P > 0.05$, *$P < 0.05$, **$P < 0.01$, ***$P < 0.001$*).

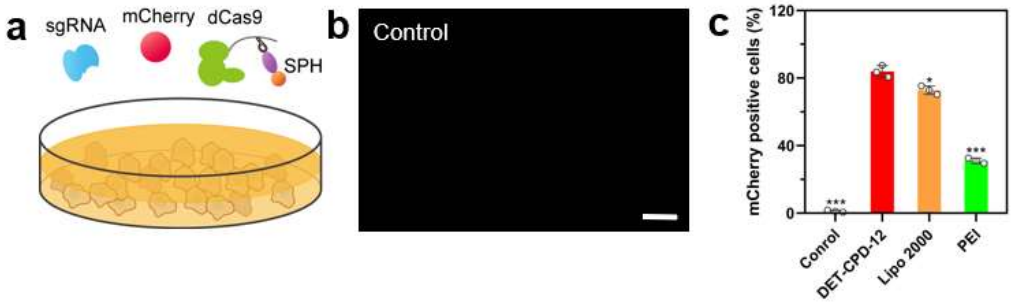


**Figure S31.** Transcriptional activation assay. (a) Illustration of CRISPR/dCas9-mediated transcriptional activation of mCherry expression after co-transfecting three plasmids (SPH, U6-sgRNA, and CMV-mCherry) by DET-CPD-12 in 293T cells for 48 h. (b) The image of 293T cells without any treatment were used as the negative control. (c) Quantitative analysis of mCherry expression in 293T cells by flow cytometry. Lipo 2000 and PEI of 25 kDa were used as the positive controls. The scale bar represents 200 μm. The error bar represents the standard error (mean ± S.D., $n$ = 3, one-way ANOVA with a Tukey post-hoc test, *$P < 0.05$, **$P < 0.01$, ***$P < 0.001$*).

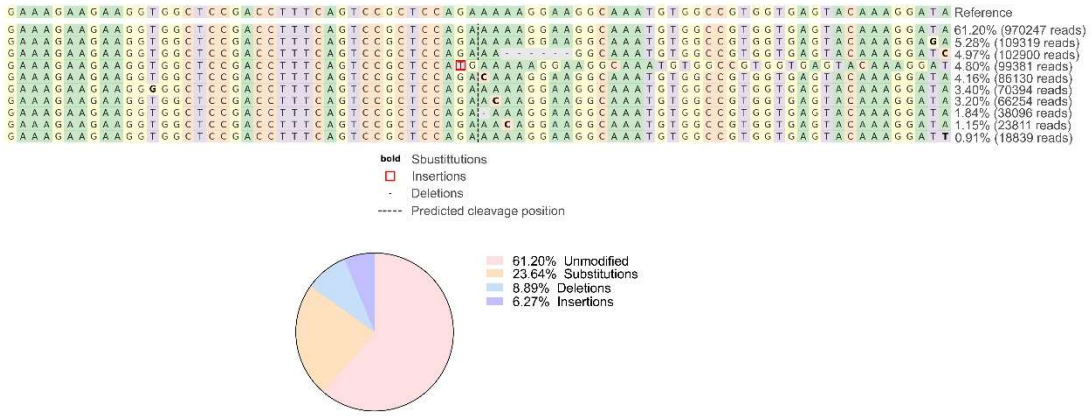


**Figure S32.** Deep-sequencing analysis of in vivo *CCNE1* mutation frequency. The mutation frequency was analyzed through a single deep-sequencing library prepared from genomic DNA pooled from 293T cells treated with DET-CPD-12/Cas9-sgCCNE1 plasmid nanocomplexes.

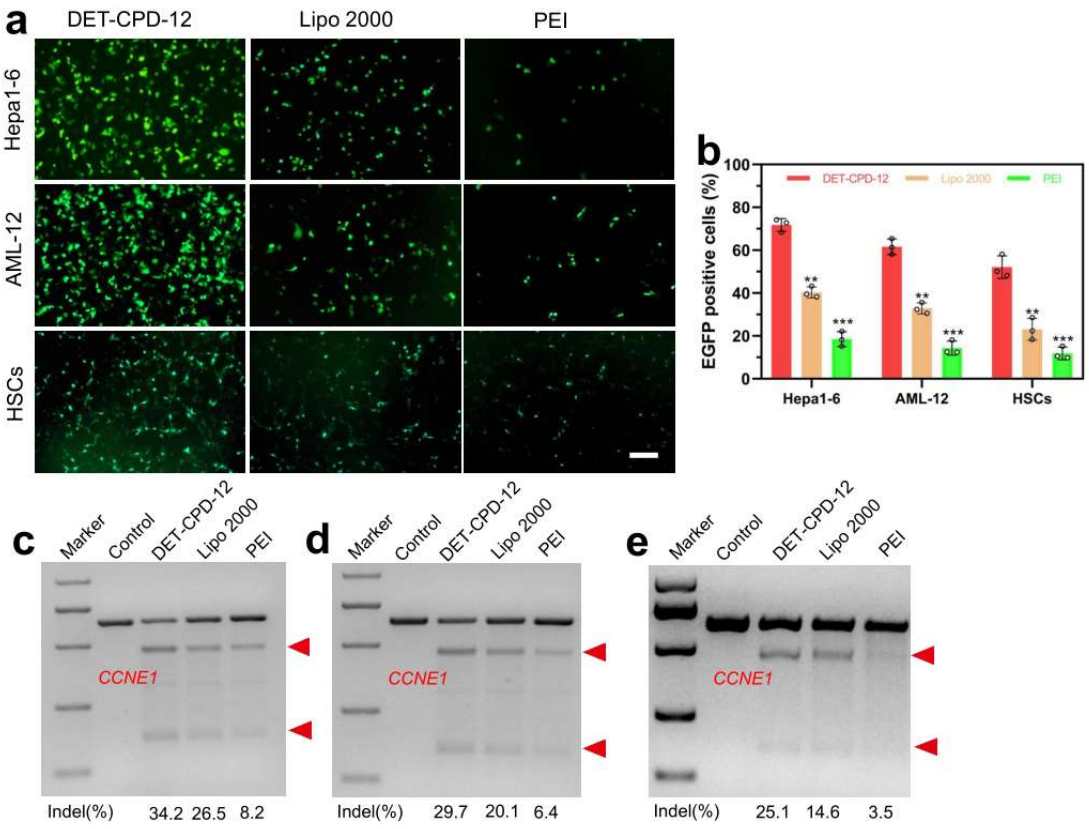


**Figure S33**. (a) The fluorescence image of GFP expression mediated by DET-CPD-12 in Hepa1-6 cells, AML-12 cells and HSCs cells for 48 h, respectively. Lipo 2000 and PEI 25 K were used as the positive controls. The scale bar represents 200 μm. (b)Flow cytometry analysis of GFP-positive cells after DET-CPD-12-mediated transfection of Cas9 plasmid in different cell lines. All quantitative data represent mean ± S. D. ($n = 3$, one-way ANOVA with a Tukey's post-hoc test, $^{**}P < 0.01$, $^{***}P < 0.001$). Analysis of indel frequency at *CCNE1* locus after the transfection of Cas9 plasmid DNA in Hepa1-6 cells (c), AML-12 cells (d) and HSCs cells (e).

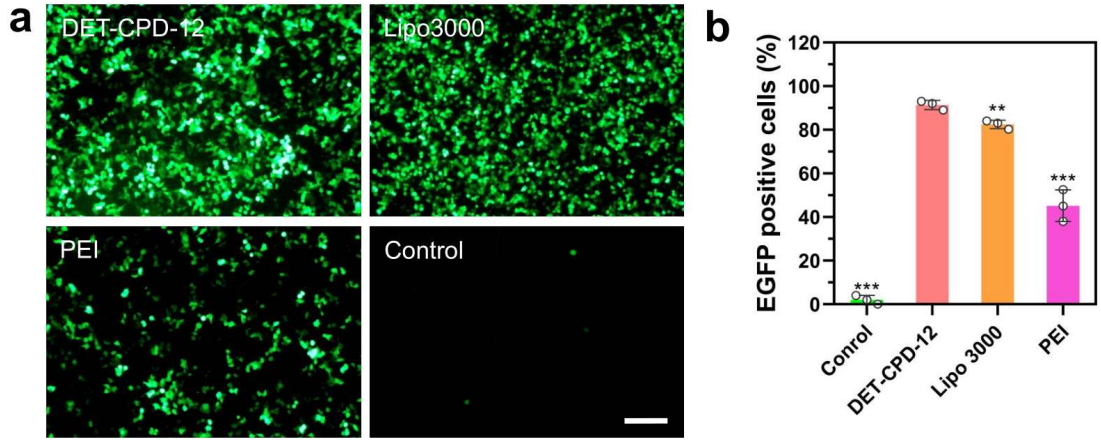


**Figure S34.** DET-CPD-12 mediated the GFP mRNA transfection. (a) EGFP expression of DET-CPD-12/mRNA-GFP nanocomplexes in 293T cells for 48 h, Lipo 3000 and PEI of 25 kDa were used as the positive controls. (b) Flow cytometry analysis of EGFP expression in the transfected cells. The scale bar represents 200 μm. The error bar represents the standard error (mean ± S.D., $n = 3$, one-way ANOVA with a Tukey post-hoc test, $^{**}P < 0.01$, $^{***}P < 0.001$).

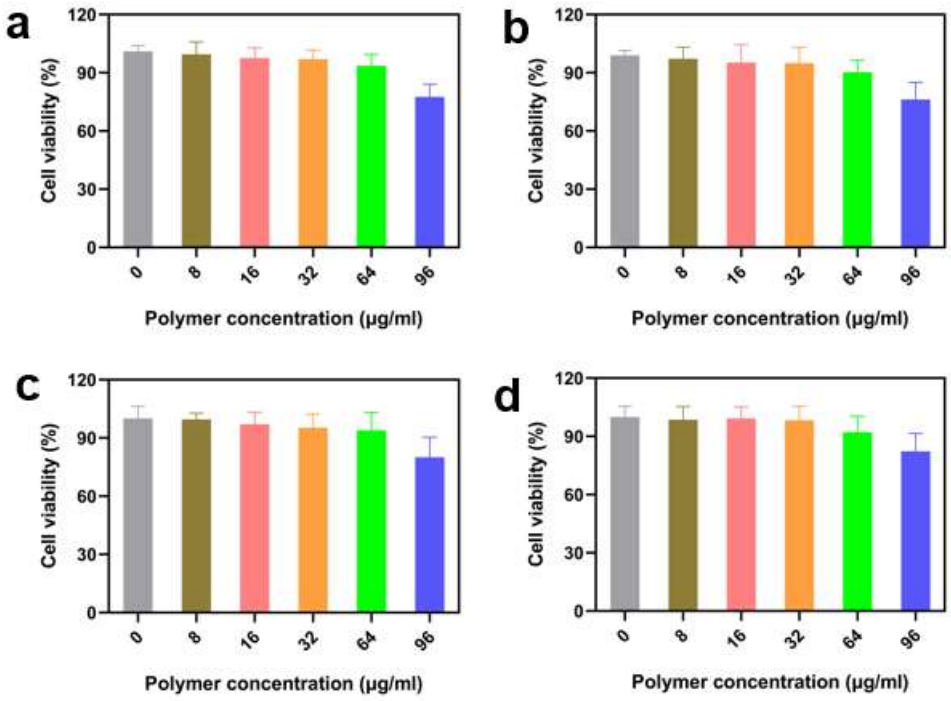


**Figure S35.** Cell viability assay. Cell viability of 293T cells (a), A549 cells (b), Hela cells (c), and HepG2 cells (d) after treatment by different concentrations of DET-CPD-12/CMV-Cas9-GFP-luciferase complexes. The concentration of DET-CPD-12 varied from 0 to 96 μg/ml, and the quantity of plasmid was fixed at 100 ng per well. Error bar represent the standard error (mean ± S.D., $n$ = 3).

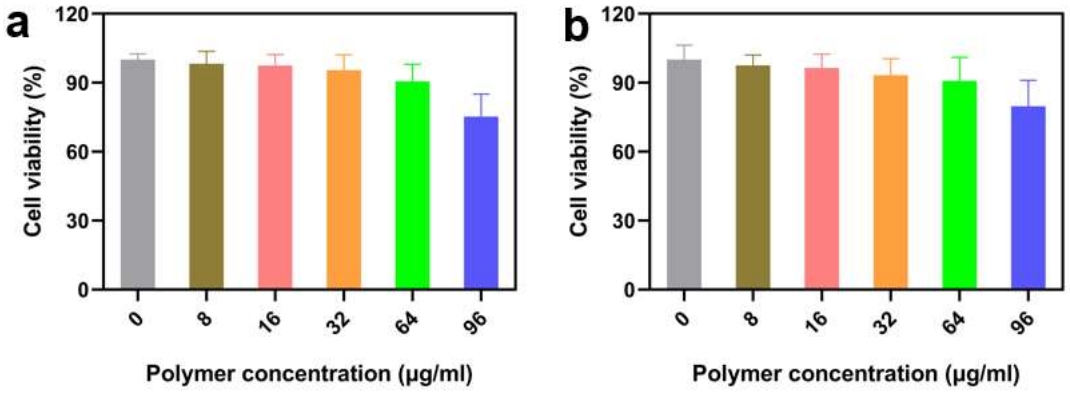


**Figure S36.** Cell viability assay. Cell viability of 293T cells after the treatment by different concentrations of DET-CPD-12/Cas9-mRNA complexes (a) and DET-CPD-12/Cas9 RNP complexes (b). The concentration of DET-CPD-12 varied from 0 to 96 μg/ml, and the amount of mRNA or RNP was fixed at 100 ng per well. Error bar represent the standard error (mean ± S.D., $n$ = 3).

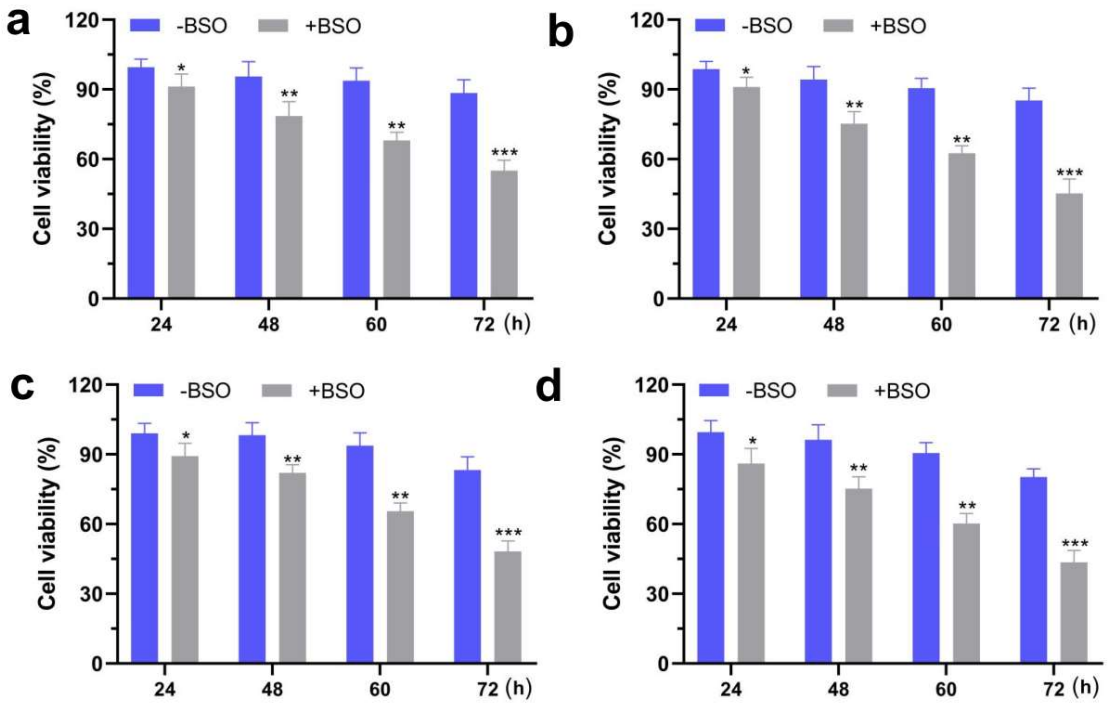


**Figure S37.** Cell viability assay after BSO treatment. Cells were treated with BSO (500 μm) for 18 h before adding the complexes solution. The other procedures were the same as the cell viability assay, and the detection time was range from 24 h, 48 h, 60 h to 72 h. The cell viability of 293T cells (a), A549 cells (b), Hela cells (c), and HepG2 cells (d) after treatment by DET-CPD-12/CMV-Cas9-GFP-luciferase complexes. The dosage of DET-CPD-12 was 0.5 μl per well, and the quantity of plasmid was fixed at 100 ng per well. Error bar represent the standard error (mean ± S.D., $n$ = 3, one-way ANOVA with a Tukey post-hoc test, *$P < 0.05$, **$P < 0.01$, ***$P < 0.001$).

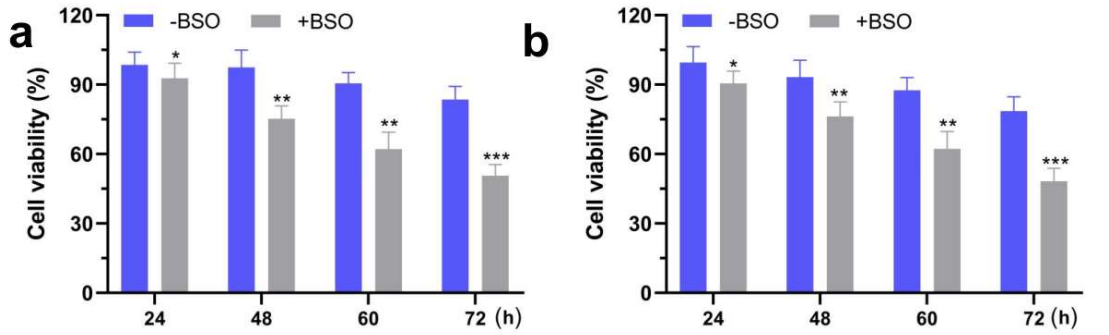


**Figure S38.** Cell viability assay after BSO treatment. Cells were treated with BSO (500 μm) for 18 h before adding the complexes solution. The other procedures were the same as the cell viability assay, and the detection time was range from 24 h, 48 h, 60 h to 72 h. Cell viability of 293T cells after the treatment by DET-CPD-12/Cas9-mRNA complexes (a) and DET-CPD-12/Cas9 RNP complexes (b). The dosage of DET-CPD-12 was 0.5 μl per well, and the amount of mRNA or RNP was fixed at 100 ng per well. Error bar represent the standard error (mean ± S.D., $n$ = 3, one-way ANOVA with a Tukey post-hoc test, *$P < 0.05$, **$P < 0.01$, ***$P < 0.001$).

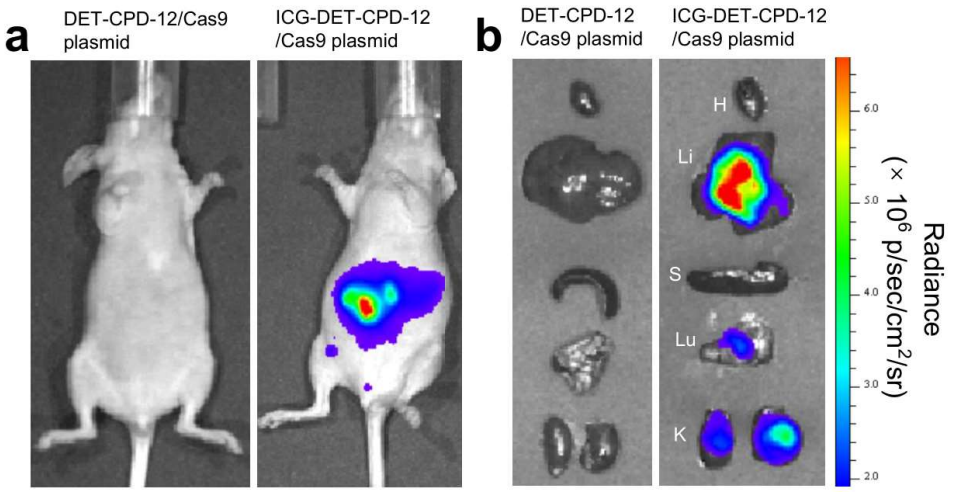


**Figure S39**. The vivo fluorescence images of the distribution of ICG-labeled DET-CPD-12/Cas9 plasmid (right) or unlabeled DET-CPD-12/Cas9 plasmid (left) in the whole mice 12 h after tail-vain administration (a), and fluorescence imaging of the dislodged organs from the treated mice (b). The left image in Figure (b) is the fluorescence image of unlabeled DET-CPD-12/Cas9 plasmid, the right image in Figure (b) is the fluorescence image of ICG-labeled DET-CPD-12/Cas9 plasmid. H, heart; Li, liver; S, spleen; Lu, lung; K, kidney.

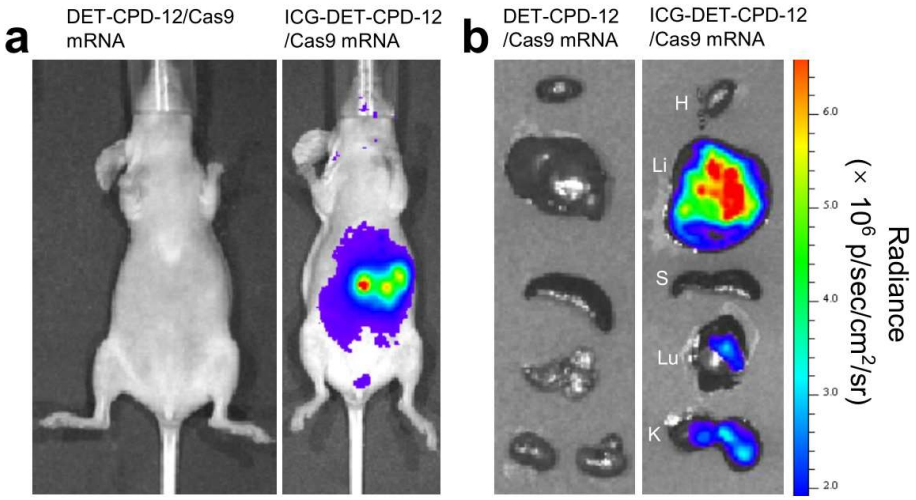


**Figure S40.** The vivo fluorescence images of the distribution of ICG-labeled DET-CPD-12/Cas9 mRNA (right) or unlabeled DET-CPD-12/Cas9 mRNA (left) in the whole mice 12 h after tail-vain administration (a), and fluorescence imaging of the dislodged organs from the treated mice (b). The left image in Figure (b) is the fluorescence image of unlabeled DET-CPD-12/Cas9 mRNA, the right image in Figure (b) is the fluorescence image of ICG-labeled DET-CPD-12/Cas9 mRNA. H, heart; Li, liver; S, spleen; Lu, lung; K, kidney.

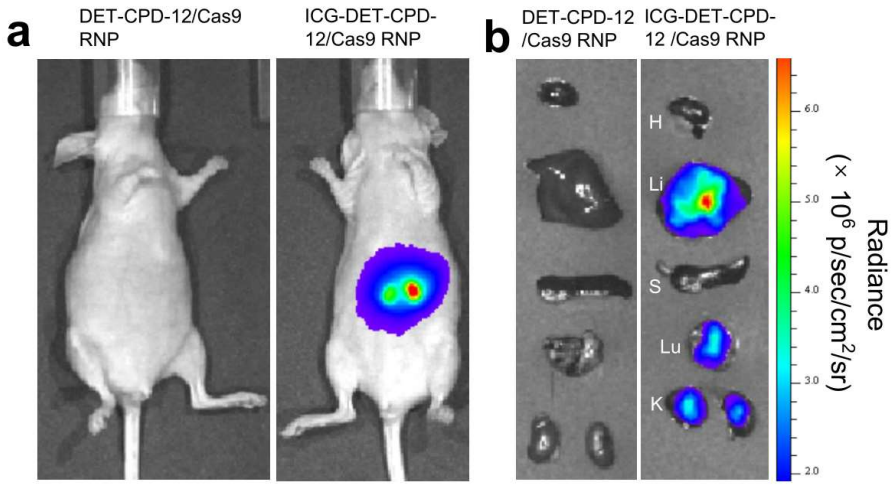


**Figure S41.** The vivo fluorescence images of the distribution of ICG-labeled DET-CPD-12/Cas9 RNP (right) or unlabeled DET-CPD-12/Cas9 RNP (left) in the whole mice 12 h after tail-vain administration (a), and fluorescence imaging of the dislodged organs from the treated mice (b). The left image in Figure (b) is the fluorescence image of unlabeled DET-CPD-12/Cas9 RNP, the right image in Figure (b) is the fluorescence image of ICG-labeled DET-CPD-12/Cas9 RNP. H, heart; Li, liver; S, spleen; Lu, lung; K, kidney.

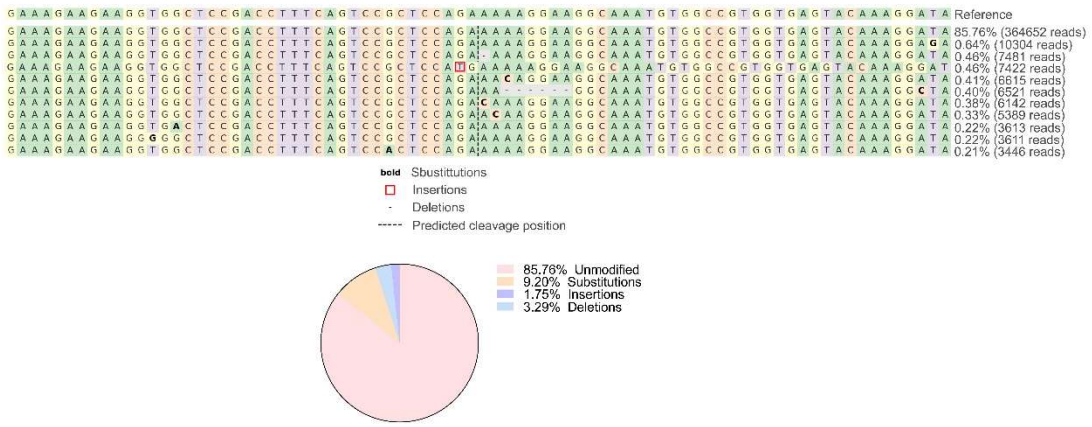


**Figure S42.** Deep-sequencing analysis of in vivo *CCNE1* mutation frequency. The mutation frequency was analyzed through a single deep-sequencing library prepared from genomic DNA pooled from APAP-treated mice treated with DET-CPD-12/Cas9-sgCCNE1 plasmid nanocomplexes.

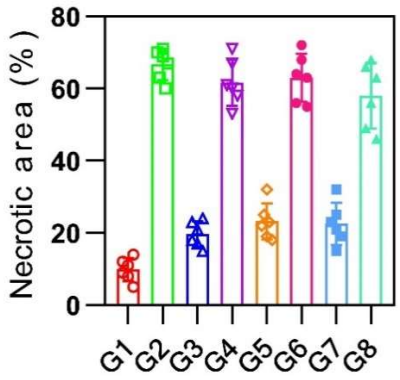


**Figure S43.** Quantification of necrotic aeras in each group by Image J software. APAP was administrated via intraperitoneal injection and DET-CPD-12/CMV-Cas9-sgCCNE1 complexes were administered via tail vein. The code denotes the follows: the code denotes the follows: G1: Mice without APAP treatment administered with PBS; G2: APAP-treated mice administered with PBS; G3: APAP-treated mice treated with DET-CPD-12/Cas9-sgCCNE1 plasmid; G4: APAP-treated mice administered with DET-CPD-12/Cas9-sgMock plasmid; G5: APAP-treated mice administered with DET-CPD-12/Cas9-sgCCNE1 mRNA; G6: APAP-treated mice administered with DET-CPD-12/Cas9-sgMock mRNA; G7: APAP-treated mice administered with DET-CPD-12/RNP-sgCCNE1; G8: APAP-treated mice administered with DET-CPD-12/RNP-sgMock. Error bars represent the standard error (mean ± S.D., $n$ = 6).

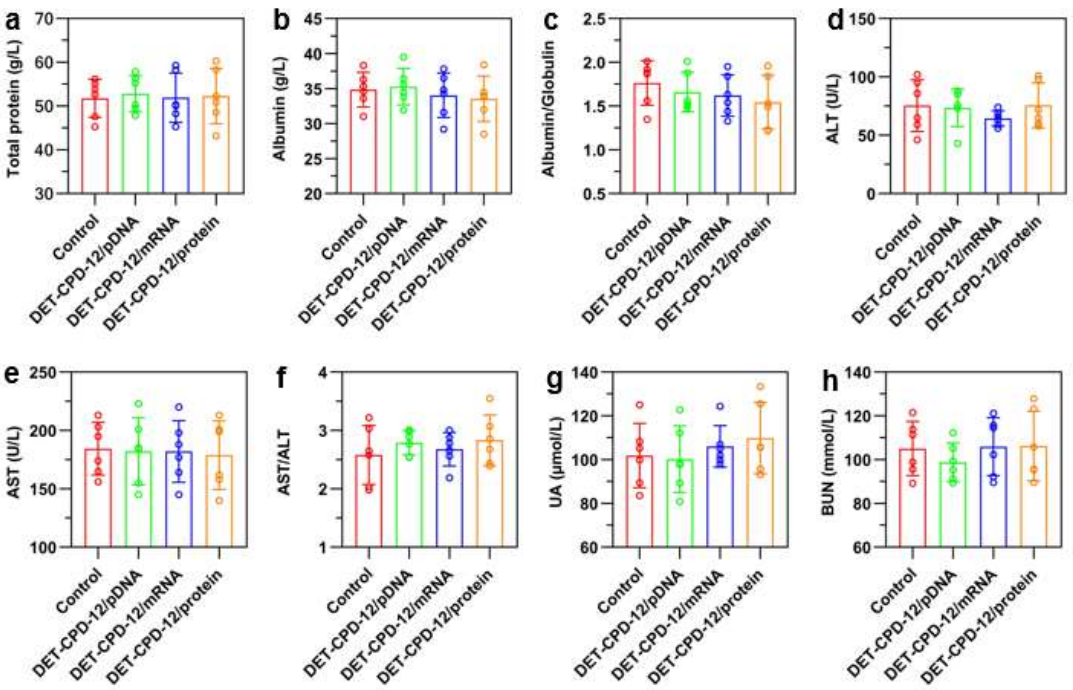


**Figure S44.** Hematological evaluation of BABL/c mice treated with DET-CPD-12/pDNA (Cas9-plasmid), DET-CPD-12/mRNA (Cas9-mRNA), DET-CPD-12/protein (Cas9 RNP) or control (saline) via tail-vein injection, respectively. The figures showed the levels of (a) total protein, (b) albumin, (c) albumin/globulin ratio, (d) ALT (alanine aminotransferase), (e) AST (aspartate aminotransferase), (f) AST/ALT ratio, (g) UA (uric acid), and (h) BUN (blood urea nitrogen) for 5 days. Error bars represent the standard error (mean ± S.D., $n$ = 6).

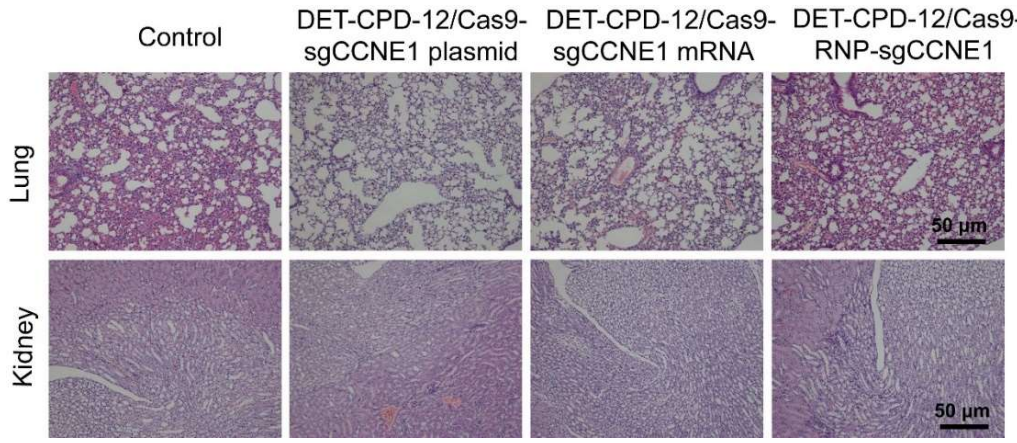


**Figure S45.** H&E staining of the lung and kidney sections from the mice after the specified treatments.

**Table S1.** The polymerization conditions and GPC characterizations of polymers.

| Poly(disulfide)s | Molar ratio [**M1**]/[**M2**] | Monomer (mM)[a] | Initiator (mM) | Time (h) | $M_n$[b] (kDa) | $M_w$[c] (kDa) | PDI |
|---|---|---|---|---|---|---|---|
| DET-1[d] | - | 2.4 | 0.03 | 0.5 | 2.29 | 2.67 | 1.16 |
| DET-2[d] | - | 2.4 | 0.03 | 1.0 | 2.58 | 2.98 | 1.15 |
| DET-3[d] | - | 2.4 | 0.03 | 1.5 | 2.73 | 3.25 | 1.19 |
| DET-4[d] | - | 2.4 | 0.03 | 2.0 | 3.13 | 3.51 | 1.12 |
| DET-5[d] | - | 2.4 | 0.03 | 2.5 | 3.21 | 4.05 | 1.26 |
| DET-6[d] | - | 2.4 | 0.03 | 3.0 | 3.34 | 4.38 | 1.31 |
| CPD-1[e] | - | 2.4 | 0.03 | 0.5 | 7.36 | 9.21 | 1.25 |
| CPD-2[e] | - | 2.4 | 0.03 | 1.0 | 8.31 | 11.5 | 1.39 |
| CPD-3[e] | - | 2.4 | 0.03 | 1.5 | 9.85 | 13.0 | 1.32 |
| CPD-4[e] | - | 2.4 | 0.03 | 2.0 | 10.5 | 13.2 | 1.26 |
| CPD-5[e] | - | 2.4 | 0.03 | 2.5 | 11.0 | 14.5 | 1.25 |
| CPD-6[e] | - | 2.4 | 0.03 | 3.0 | 11.5 | 14.7 | 1.28 |
| DET-CPD-1 | 1:1 | 2.4 | 0.03 | 1.5 | 6.78 | 10.9 | 1.61 |
| DET-CPD-2 | 1:2 | 2.4 | 0.03 | 1.5 | 7.48 | 9.89 | 1.32 |
| DET-CPD-3 | 2:1 | 2.4 | 0.03 | 1.5 | 7.51 | 9.79 | 1.31 |
| DET-CPD-4 | 1:2 | 2.4 | 0.03 | 0.5 | 6.28 | 7.36 | 1.17 |
| DET-CPD-5 | 1:2 | 2.4 | 0.03 | 1.0 | 6.75 | 8.57 | 1.30 |
| DET-CPD-6 | 1:2 | 2.4 | 0.03 | 2.0 | 8.45 | 11.5 | 1.36 |
| DET-CPD-7 | 1:2 | 2.4 | 0.03 | 2.5 | 8.98 | 12.3 | 1.37 |
| DET-CPD-8 | 1:2 | 2.4 | 0.03 | 3.0 | 9.17 | 13.1 | 1.42 |
| DET-CPD-9 | 1:2 | 2.4 | 0.12 | 1.5 | 2.80 | 3.52 | 1.26 |
| DET-CPD-10 | 1:2 | 2.4 | 0.06 | 1.5 | 5.74 | 6.98 | 1.22 |
| DET-CPD-11 | 1:2 | 2.4 | 0.015 | 1.5 | 19.1 | 26.7 | 1.40 |
| DET-CPD-12[f] | 1:2 | 2.4 | 0.03 | 1.5 | 8.70 | 10.8 | 1.24 |

[a]Total concentration of monomers; [b]Number average molecular weight (kDa) from GPC profiles; [c]Mass average molecular weight (kDa) from GPC profiles; [d]**M1** as the monomer for DETs; [e]**M2** as the monomer for CPDs; [f]$PEG_{2000}$-SH as the initiator.

**Table S2.** Primer sequences for sgRNA synthesis used in this study.

| Primer names | Sequences (5'-3') |
|---|---|
| sgCCNE1 | TTTCAGTCCGCTCCAGAAAA |

**Table S3.** Primer sequences for PCR amplification of target genes.

| Primer names | Sequences (5'-3') |
|---|---|
| CCNE1-F | TCCAAGCCCAAGTCCTGAGCCA |
| CCNE1-R | TGGCCTGCAGCTCTGTTTTGGG |

**Table S4.** Sequences of off-target sites estimated by Cas-OFFinder and their targeting location in the chromosome.

| Nucleic Acid ID | Sequences (5'-3') | Locations in chromosomes |
|---|---|---|
| CCNE1-off1 | TTTCAaTCCtCTaCAGAAAA | chr5: 105878066 |
| CCNE1-off2 | aTTCtGTCaGCTCCAGAAAA | chr5: 139541446 |
| CCNE1-off3 | TTTCAGTCCGCTgCAGgAcA | chr7: 128389411 |
| CCNE1-off4 | TTcCAGTCCaCaCCAGAAAA | chr2: 15573778 |
| CCNE1-off5 | TTTCAGTCCctTCCAGAAAg | chr2: 48525573 |
| CCNE1-off6 | TTTCAGTCtGCTgCAtAAAA | chr16: 52144864 |
| CCNE1-off7 | TcTCAGTtCGaTCCAGAAAA | chr9: 92065850 |

**Table S5.** Primer sequences for PCR amplification of off-target sites.

| Nucleic Acid ID | Sequences (5'-3') |
|---|---|
| CCNE1-off1-F | CCCCATTTTCCCTCCTATTCTTCCACA |
| CCNE1-off1-R | TGGTGGCTACGGATGGGCTGT |
| CCNE1-off2-F | ACACGCCAATCTGAAGGCCAGG |
| CCNE1-off2-R | GGCGCGTGCTTCGGAATACA |
| CCNE1-off3-F | AGTGGCAATCCAGCATGACCCG |
| CCNE1-off3-R | TCCAGGGCACCTGCACATTCCT |
| CCNE1-off4-F | TCCGTGCCCAAGGTACCCCTTT |
| CCNE1-off4-R | TGCCAGCTACCCACAAAACCCG |
| CCNE1-off5-F | TGCCATCCCACAGAAAGGATTGC |
| CCNE1-off5-R | AGGGTGGTTCCTGTGGCAGT |
| CCNE1-off6-F | ACCTTGTAGCCTAAGGTGGGTCTTT |
| CCNE1-off6-R | AGCTGTGGTAACGTAAGGGGCA |
| CCNE1-off7-F | ATGTGCCAGGCTGTGGGTGA |
| CCNE1-off7-R | TCAAGCGTTCCCCGCTGTCCTA |

**Table S6.** Deep-sequencing analysis of CCNE1 off-target sites.

| Nucleic Acid ID | Total reads | Non-edited (%) | Mutation (%) |
|---|---|---|---|
| CCNE1-off1 | 342229 | 93.89 | 0.88 |
| CCNE1-off2 | 783204 | 95.48 | 0.34 |
| CCNE1-off3 | 1052018 | 97.70 | 0.18 |
| CCNE1-off4 | 953012 | 98.14 | 0.12 |
| CCNE1-off5 | 560213 | 96.39 | 0.56 |
| CCNE1-off6 | 456755 | 97.40 | 0.19 |
| CCNE1-off7 | 652024 | 96.63 | 0.24 |